Voronoi and Delaunay cells of root lattices: classification of their faces and facets by Coxeter-Dynkin diagrams

1992 J. Phys. A: Math. Gen. 25 5089

(http://iopscience.iop.org/0305-4470/25/19/020)

J. Phys. A: Math. Gen. 25 (1992) 5089–5134. Printed in the UK

Voronoi and Delaunay cells of root lattices: classification of their faces and facets by Coxeter–Dynkin diagrams

R V Moody† and J Patera‡

† Department of Mathematics, University of Alberta, Edmonton, Alberta T6G 2G1, Canada

‡ Centre de recherches mathématiques, Université de Montréal, CP 6128–A, Montréal, Québec H3C 3J7, Canada

Received 16 March 1992, in final form 2 June 1992

Abstract. The Voronoi domains, their duals (Delaunay domains) and all their faces of any dimension are classified and described in terms of the Weyl group action on a representative of each type of face. The representative of a face type is specified by a decoration of the corresponding Coxeter–Dynkin diagram. The rules of domain description are uniform for root lattices of simple Lie groups of all types. An explicit description of the representatives of all faces is carried out for the domains of root lattices of the four classical series and for the five exceptional simple Lie groups. The Coxeter–Dynkin diagrams required here are the diagrams extended by the highest *short* root. Each diagram is partitioned into two subdiagrams, one describing completely a d-face of the Voronoi domain, its complement completely describing the dual of the d-face. The applicability of our classification method to generalized kaleidoscopes is explained.

In memory of Hans Zassenhaus

1. Introduction

The purpose of this article is to study the Voronoi domains of the root lattices of the simple Lie groups of all ranks $n \geqslant 1$, to classify and to describe their faces of all dimensions d (d-faces) for $0 \leqslant d < n$, and to give a similar description of their duals or Delaunay domains [1, 2].

In physics literature, particularly when one is concerned with dimensions not greater than three, these domains are also called Wigner–Seitz cells and Brillouin zones. Other occasionally used names are proximity cells and Dirichlet domains.

In general, for a lattice Γ in $\mathbb{R}^n$, the Voronoi domain, or cell, of a lattice point α, denoted by $V(\alpha)$, is the set of all points of $\mathbb{R}^n$ that are at least as close to α as to any other point of Γ.

Voronoi cells appear naturally in problems of crystallography, solid state physics, coding theory and, most recently, in the theory of quasicrystals. Our interest in the Voronoi cells of root lattices was awakened by the work of P Kramer *et al* [3], in which these cells and their duals play a crucial role.

Information about the Voronoi cells of root lattices of dimension greater than three is scattered about the literature. A detailed account of the lattices A_4, D_4, and

0305-4470/92/195089+46$04.50

D_6 is given in a series of papers [3, 4]. The most detailed account of the Voronoi cells of root lattices appears in the excellent paper of Conway and Sloane [5, 6], where the direct motivation is coding theory and sphere packing. Much information on four-dimensional crystallography is found in [7, 8]. For an informative introduction to the importance of Voronoi cells in the theory of lattices see [9].

In this paper we start from the result of Conway and Sloane (equation (2.28)) in the case of Voronoi cells and from the Wythoff prescription (equation (4.44)) for Delaunay cells and develop a simple graph-theoretical method of simultaneously classifying the facet structure of both cells. The method also gives explicit information on the symmetries of each facet, its vertices, and other subfacets. In spirit it is similar to the methods of Coxeter [10] and indeed it relies on the affine Coxeter–Dynkin diagrams and the remarkable properties of the affine Weyl group and its fundamental region.

The classification of the faces and facets of the Voronoi and Delaunay domains is encoded in certain 'decorated' versions of these same diagrams. The facet structure of the Voronoi cells is described by a series of decorations of the corresponding Coxeter–Dynkin diagram and an algorithm for proceeding from d-facets to $(d-1)$-facets. The dual (Delaunay) cells are described simultaneously from the same diagram although the interpretation of the nodes of the diagram referring to facets of the Voronoi and Delaunay domains is different.

Since the root lattice of a simple Lie algebra is, in fact, generated by its short roots, a multi-length root system gives rise to Voronoi and Delaunay cells that also occur in the analysis of the root system comprised by its short roots (this is clearly visible in the A_2 and G_2 case in figure 1). Our method works using both the diagrams of the full root system and its short root subsystem. It is interesting and revealing to see how the information given in each case both coincides and differs. The differences are due to the differences in the Weyl groups and how much of the facial symmetry is carried by these groups.

Of particular interest in the classification are the vertices of the Voronoi domains, sometimes called the *holes* of the root lattice. Locally these are the points of $\mathbb{R}^n$ most distant from all the nearest lattice points. In general, a root lattice has several types of holes as classified up to equivalence by the affine Weyl group. More precisely, there are n, 1, 2, 3, 2, 2, 2, 1, 1 W-orbits of holes respectively in the root lattices A_n $(n \geqslant 1)$, $B_n, (n \geqslant 2)$, $C_n, (n \geqslant 3)$, $D_n, (n \geqslant 4)$, E_6, E_7, E_8, F_4, and G_2. If the Weyl group is extended by the symmetries of the Coxeter–Dynkin diagram, then the number of different types of holes in the root lattices $A_n, (n \geqslant 2)$, D_4, $D_n, (n \geqslant 5)$, and E_6 reduces to $[(n+1)/2]$, 1, 2, 1 respectively.

We assume that the reader is familiar with the properties of root and weight lattices of the simple Lie groups, their classification, extended or affine Coxeter–Dynkin diagrams, the affine Weyl group, etc. A basic reference is [11].

In section 2 we recall some pertinent facts of the theory, setting up the notation and fixing the terminology.

Section 3 contains the elementary examples of A_2, B_2 and G_2 of two-dimensional root lattices and serves to orient the reader to the way in which we relate facets to decorated diagrams and to illustrate the concise way necessary to provide the information about the domains in the general case. The last example, C_4, demonstrates how all details about the faces can be obtained from the classification that we provide here.

Section 4 contains the theoretical justification of the method. Section 5 contains

our results about the Voronoi and Delaunay domains in A_n, B_n, C_n, D_n, E_6, E_7, E_8, F_4 and G_2. The main results of the article are summarized in tables 4–12.

In section 6 we briefly indicate how our method is applicable to generalized kaleidoscopes in spherical, Euclidean or hyperbolic spaces. We confine our discussion to a few examples. The generalization is fullly developed in a subsequent paper [12]. It provides a new proof of the classification described here which applies to any W-orbit of points in a generalized kaleidoscope and allows us to extend our results to include the classification of Voronoi and Delaunay cells of all the weight lattices of the semi-simple Lie group.

After this manuscript was submitted we were made aware of [6]. This paper contains a case-by-case description of the Voronoi and Delaunay cells of the root and weight lattices of A_n, D_n, E_6, E_7, E_8. It is, however, very different in spirit from our paper. The conclusions of [6] clearly reveal the unity of the description of Voronoi and Delaunay domains (and to a lesser degree their facets) in terms of Coxeter–Dynkin diagrams. However, the fundamental duality between facets and dual facets is not observed. Nor does the proof, which depends on explicit knowledge of each lattice individually, reveal the underlying unity. In particular the extension to other W-orbits in Euclidean and non-Euclidean spaces is not within the scope of [6].

For convenience we summarize here our algorithm for classifying the Voronoi and Delaunay cells.

We assume we have a root lattice Q generated by a root system Δ whose Coxeter–Dynkin diagram is called CD and whose Weyl group is W.

(i) Dualize CD, form the extended dual CD, and redualize. Call the new diagram N and write the extention node as $\odot$ (see the root lattice diagrams in table 1).

(ii) At each step N is partitioned into two subgraphs

$$N = N^d_{\text{Vor}} + N^{n-d}_{\text{Del}}. \tag{1.1}$$

Nodes of N^d_{Vor} are drawn as boxes, nodes of N^{n-d}_{Del} are circles. N^d_{Vor} has $d+1$ nodes. The subgraph N^{n-d}_{Del} is always connected and always contains $\odot$. Every such partition describes a different d-dimensional face of $V(0)$ and its dual of dimension $n-d$. In spite what the notation suggests there may be several permissible partitions of N for a given d. These give rise to different W-equivalence classes of facets.

(iii) Boxes which are not joined by an edge of N to any node of N^{n-d}_{Del} are marked with a cross, $\times$.

(iv) The subdiagram N^d_{Vor} stands for the properties of a d-face of the Voronoi cell $V(0)$ and also its W-orbit. The $d+1$ boxes of the N^d_{Vor} stand for vertices of a d-simplex $\mathcal{S}^d$ (a d-face of the affine fundamental chamber) and the crosses in boxes stand for the reflections that generate the group of symmetries G^d (in the Weyl group W) of the d-face. The full d-face is the union of the images of $\mathcal{S}^d$ under G^d.

(v) The subdiagram N^{n-d}_{Del} stands for the $(n-d)$-face of the Delaunay cell that is dual to the cell of Voronoi given by N^d_{Vor}. In particular for $d=0$, the subgraph N^0_{Vor} contains a single box and stands for a vertex of $V(0)$, while N^n_{Del} describes the corresponding Delaunay cell.

(vi) When $d=n$, we have $N^n_{\text{Vor}} = N$; all nodes are boxes and all but the extension node are decorated by the cross. The diagram describes then the properties of the Voronoi cell $V(0)$ centred at the origin (see table 1). When $d=-1$, we have $N^{n+1}_{\text{Del}} = N$; all nodes are circles, only the extension node is dotted. The diagram describes the properties of the whole root lattice (see table 1).

Table 1. Lattice diagrams with numbering of nodes, decorated diagrams of the Voronoi cell $V(0)$ with marks and orders of the Weyl group.

Type	Root lattice diagram with numbering of nodes	V(0) diagram with marks	Weyl group order
A_n $n\geq 2$	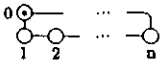	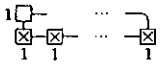	$(n+1)!$
B_n $n\geq 2$	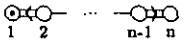		$2^n n!$
C_n $n\geq 3$	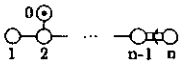	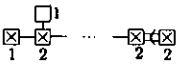	$2^n n!$
D_n $n\geq 4$	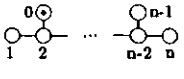	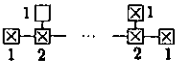	$2^{n-1} n!$
E_6	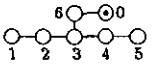	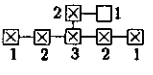	$2^7 3^4 5$
E_7	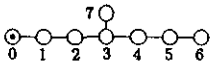	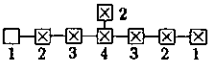	$2^{10} 3^4 5\ 7$
E_8	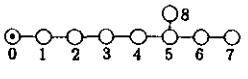	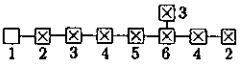	$2^{14} 3^6 5^2 7$
F_4	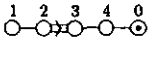	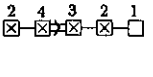	$2^7 3^2$
G_2			$2^2 3$

(vii) Lower-dimensional facets of $V(0)$, their duals, and the multiplicities of their occurrence are determined by successively replacing boxes from N^n_{Vor} by circles (subject to the conditions (ii) and (iii)). If there are several choices for replacement of boxes by circles, each choice leads to a different W-equivalence class of facets and their duals.

Moreover, the algorithm (i)–(vii) can be used to find the facets of facets of Voronoi and Delaunay cells and their multiplicities (see section 4.7). One simply applies the algorithm to the corresponding subgraph N^d_{Vor} or N^{n-d}_{Del}, partitioning the subgraph into two parts (this requires a convention on how to draw two types of boxes or circles) subject to the requirements of the algorithm, etc.

2. Notation and setting up the problem

Let $\mathbf{A} = (A_{ij})_{1\leqslant i,k\leqslant n}$ be an indecomposable Cartan matrix, V and $\check{V}$ vector spaces of dimension n over $\mathbb{R}$, and Π and $\check{\Pi}$ are bases of V and $\check{V}$ respectively,

$$\Pi = \{\alpha_1, \alpha_2, \ldots, \alpha_n\} \qquad \check{\Pi} = \{\check{\alpha}_1, \check{\alpha}_2, \ldots, \check{\alpha}_n\}. \tag{2.1}$$

There is a unique bilinear form

$$\langle \cdot , \cdot \rangle : V \times \check{V} \to \mathbb{R} \tag{2.2}$$

defined by

$$\langle \alpha_i, \check{\alpha}_j \rangle = A_{ij}. \tag{2.3}$$

Let W denote the Weyl group of the Cartan matrix **A**. The group W is generated by its elements $r_1, \ldots, r_n$,

$$W = \langle r_1, \ldots, r_n \rangle. \tag{2.4}$$

It acts faithfully both on V and $\check{V}$. One has

$$r_i \alpha_j = \alpha_j - A_{ji} \alpha_i \tag{2.5a}$$

$$r_i \check{\alpha}_j = \check{\alpha}_j - A_{ij} \check{\alpha}_i. \tag{2.5b}$$

Here r_i is the reflection in the hyperplanes

$$H_{\check{\alpha}_i} := \{ x \in V | \langle x, \check{\alpha}_i \rangle = 0 \} \tag{2.6a}$$

or

$$H_{\alpha_i} := \{ x \in \check{V} | \langle \alpha_i, x \rangle = 0 \} \tag{2.6b}$$

according to which side of $\langle \cdot , \cdot \rangle$ we look at.

The bilinear form $\langle \cdot , \cdot \rangle$ is W-invariant:

$$\langle wv, wv' \rangle = \langle v, v' \rangle$$

for all $w \in W$, for all $(v, v') \in V \times \check{V}$.

The W-transforms of Π and $\check{\Pi}$,

$$\Delta := W\Pi \qquad \text{and} \qquad \check{\Delta} := W\check{\Pi} \tag{2.6}$$

are the finite root systems defined by Π and $\check{\Pi}$; Π and $\check{\Pi}$ are the corresponding simple roots. The unique positive definite symmetric W-invariant bilinear form,

$$(\cdot \mid \cdot) : V \times V \to \mathbb{R} \tag{2.7}$$

on V is defined by the two properties

$$\frac{2(\alpha_i \mid \alpha_j)}{(\alpha_j \mid \alpha_j)} = A_{ij} \tag{2.8a}$$

$$(\alpha \mid \alpha) = 2 \qquad \text{for all long roots.} \tag{2.8b}$$

The bilinear form $(\cdot \mid \cdot)$ defines a Euclidean metric on V

$$\mathrm{d}(x, y) = |x - y| = (x - y \mid x - y)^{1/2} \tag{2.9}$$

relative to which each r_i is an orthogonal reflection.

It is useful to fix, once and for all, a numbering system for simple roots. We adopt the Dynkin numbering which is shown in table 1 together with the orders of the Weyl groups.

Using $(\cdot \mid \cdot)$ we identify V and $\check{V}$ so that

$$\frac{2\alpha_j}{(\alpha_j \mid \alpha_j)} \longleftrightarrow \check{\alpha}_j . \tag{2.10}$$

In general, there is a bijection

$$\check{}: \Delta \longleftrightarrow \check{\Delta} \tag{2.11}$$

that is W-invariant and satisfies

$$\frac{2\alpha}{(\alpha \mid \alpha)} \longleftrightarrow \check{\alpha} \tag{2.12}$$

under the isomorphism of V and $\check{V}$. We define $\check{\alpha} \in V$ for all non-zero $\alpha \in Q$ by (2.12).

Relative to Π, the root system Δ has a highest root ξ and a highest short root ξ_s. (If Δ has only one root length then $\xi = \xi_s$). Then $\check{\xi}$ and $\check{\xi}_s$ are respectively the highest short root and the highest long root of $\check{\Delta}$.

The lattices generated in V by Δ and $\check{\Delta}$ are

$$Q = \sum_{i=1}^{n} \mathbb{Z}\alpha_i = \sum_{\alpha_i \text{short}} \mathbb{Z}\alpha_i \tag{2.13}$$

$$\check{Q} = \sum_{i=1}^{n} \mathbb{Z}\check{\alpha}_i = \sum_{\check{\alpha}_i \text{short}} \mathbb{Z}\check{\alpha}_i . \tag{2.14}$$

The second equalities are both well known and easy to show. Both Q and $\check{Q}$ are W-invariant.

Our task is to describe the structure of the Voronoi cells of Q. By definition, for $\alpha \in Q$, the Voronoi cell $V(\alpha)$ around α is

$$V(\alpha) := \{x \in V \mid |x - \alpha| \leqslant |x - \beta|, \text{ for all } \beta \in Q\}. \tag{2.15}$$

Obviously $V(\alpha) = V(0) + \alpha$ for all $\alpha \in Q$ and $V(0)$ is W-invariant. We wish to determine the W-orbits of the vertices, edges, 2-facets, ..., $(n-1)$-facets of $V(0)$. We will reserve the term 'face' for the $(n-1)$-facets of $V(0)$. We make the convention that facets are closed, so a facet contains various subfacets of lower dimension. We will see that our algorithm for extracting the information will begin by a description of the faces and work by descending dimension to the remaining facets. As we have pointed out, the same Voronoi cells may be determined by different root lattices since it is only short roots that are involved. However, the Weyl groups are different and so we obtain different information about the symmetry of the facets by using different root systems.

An important cellular decomposition of V associated with the Voronoi cells is the decomposition into dual cells. If f is a facet of a Voronoi cell $V(\beta)$ then the (metrical) dual f^* of f is the convex hull of the lattice points $\beta \in Q$ for which f is a facet of $V(\beta)$. Equivalently, f^* is the convex hull of the lattice points β that are closest to f. We will obtain a description of the dual facets f^* simultaneously with that of the facet f.

The extended Weyl groups are $W \ltimes Q$ and $W \ltimes \check{Q}$, where the action of W on Q and $\check{Q}$ are given by (2.5). The action of

$$W_a := W \ltimes Q \tag{2.16a}$$

on V (which is the only one we have need of here) is given by letting Q act by translation on V:

$$(w, q): \ x \longmapsto wx + q. \tag{2.16b}$$

The affine Weyl group $W \ltimes Q$ is generated by $r_1, r_2, \ldots, r_n$ and by an additional affine reflection

$$r_0 : x \longmapsto x + (1 - \langle x, \check{\xi}_s \rangle)\xi_s$$

$$r_0 x = x + \left\{1 - \frac{2(x \mid \xi_s)}{(\xi_s \mid \xi_s)}\right\} \xi_s. \tag{2.17}$$

Note that defining

$$\overline{r_0}: \ x \longmapsto x - \langle x, \check{\xi}_s \rangle \xi_s \tag{2.18}$$

we have $\overline{r_0} \in W$ and

$$r_0 \overline{r_0}: \ x \longmapsto x + \xi_s \qquad \text{for all } x \tag{2.19}$$

i.e. $r_0 \overline{r_0}$ is the translation by $\xi_s \in Q$. The region F,

$$F := \{x \in V \mid \langle x, \check{\alpha}_i \rangle \geqslant 0, i = 1, 2, \ldots, n, \text{ and } \langle x, \check{\xi}_s \rangle \leqslant 1\} \tag{2.20}$$

is a *fundamental region* for the action of W_a on V. In fact [B, ch V, section 3]

(i) $\bigcup_{w \in W_a} wF = V$,
(ii) if $x \in F, w \in W_a$ then $wx \in F \Longleftrightarrow wx = x$,
(iii) if $x \in F$ then $\mathrm{Stab}_{W_a}(x)$ is generated by the reflections in the walls of F containing x.

Define the *fundamental weights* $\omega_1, \omega_2, \ldots, \omega_n \in V$ by

$$\langle \omega_i, \check{\alpha}_j \rangle = \delta_{ij} \tag{2.21}$$

and the weight lattice P,

$$P = \sum_{i=1}^{n} \mathbb{Z}\omega_i. \tag{2.22}$$

The coefficients $\{m_0, m_1, \ldots, m_n\}$ in

$$\check{\xi}_s = \sum_{i=1}^{m} m_i \check{\alpha}_i \tag{2.23}$$

together with $m_0 = 1$ are the *marks* of the dual root system $\check{\Delta}$. Their values are shown in table 1. For all i, we have $m_i \in \mathbb{Z}_+$.

Lemma 1. F is the convex hull of 0 and

$$\left\{\frac{\omega_1}{m_1}, \frac{\omega_2}{m_2}, \ldots, \frac{\omega_n}{m_n}\right\}. \tag{2.24}$$

Proof. $\{\omega_1/m_1, \omega_2/m_2, \ldots, \omega_n/m_n\}$ is a basis of V. Let $x \in V$ be written as $x = \sum c_i \omega_i / m_i$. Then

$$\langle x, \check{\alpha}_j \rangle \geqslant 0 \Longleftrightarrow c_j \geqslant 0.$$

$$\langle x, \check{\xi}_s \rangle \leqslant 1 \Longleftrightarrow \sum \frac{c_i}{m_i} m_j \langle \omega_i, \check{\alpha}_j \rangle = \sum c_i \leqslant 1. \tag{2.25}$$

□

We will be primarily interested in the boundary F_0 of F,

$$F_0 := \left\langle \frac{\omega_1}{m_1}, \frac{\omega_2}{m_2}, \ldots, \frac{\omega_n}{m_n} \right\rangle_{\text{conv}}. \tag{2.26}$$

It lies in the affine hyperplane

$$H_0 := \{x \in V \mid \langle x, \check{\xi}_s \rangle = 1\}. \tag{2.27}$$

Given two subsets S and T of V, we say that S *supports* T (and T supports S) if the affine spans of S and T are equal. For example F_0 and H_0 support each other.

In terms of F we have the following description of $V(0)$ due to Conway and Sloane [5]. We include a proof here because it is an essential step in our argument.

Lemma 2. [5, ch 21]

$$V(0) = WF := \bigcup_{w \in W} wF. \tag{2.28}$$

Proof. Let $x \in F$. We claim that for all $\alpha \in Q$, $|x| \leqslant |x - \alpha|$.

Indeed, since whenever a reflecting hyperplane H separates x and α we have $|x - r_H \alpha| \leqslant |x - \alpha|$, we can assume $\alpha \in F$. However, by (2.20), $Q \cap F = \{0\}$, so $\alpha = 0$.

Now let $x \in V(0)$. To prove that $x \in WF$ we may assume that x lies in

$$C := \{x \in V \mid \langle x, \check{\alpha}_i \rangle \geqslant 0\} \tag{2.29}$$

which is a fundamental domain for the action of W on V. Then for all $\beta \in Q$,

$$|x| \leqslant |x - \beta| \Longleftrightarrow \langle x, \check{\beta} \rangle \leqslant 1.$$

In particular, $\langle x, \check{\xi}_s \rangle \leqslant 1 \Longrightarrow x \in F$. Thus $V(0) \subset WF$. Conversely $x \in F \Longrightarrow x \in V(0)$ and so we see that $WF \subset V(0)$. □

A concise way to provide essential information about $V(0)$ is by means of the decorated diagrams of table 1.

During the subsequent computations one frequently needs to use the following relations,

$$\alpha = A\omega \Longleftrightarrow \alpha_i = \sum A_{ij}\omega_j \tag{2.30}$$

$$\omega = A^{-1}\alpha \Longleftrightarrow \omega_i = \sum (A^{-1})_{ij}\alpha_j \tag{2.31}$$

$$r_i\omega_k = \omega_k - \delta_{ik}\alpha_k \qquad i,j,k = 1,2,\ldots,n \tag{2.32}$$

which are simple consequences of (2.5), (2.8), (2.10) and (2.21). The list of Cartan matrices **A** can be found in many places [11, 13, 14], their inverses are found for example in [14].

The Euler formula [10] which relates the numbers N_d of d-facets,

$$\sum_{d=0}^{n-1} N_d = 1 - (-1)^n \tag{2.33}$$

offers a useful verification of our counting of the facets of Voronoi and Delaunay cells.

3. Introductory examples: A_2, B_2, G_2 and C_4

In this section we consider two types of examples. The first are the two-dimensional root lattices of the simple Lie groups A_2, $B_2(\cong C_2)$, and G_2. Their Voronoi domains are most easily described by simply drawing them (figure1) using only the definition. This elementary situation allows us to illustrate our concise notation for the same results; in particular, the two interpretations of the decoration of the diagram required for description of the facets and their duals. In each successive case we adopt more of the view point that is used in the rest of the paper.

Our second type of example is C_4. We use it also further on in section 4 and also in illustrating the generalized kaleidoscope in section 6. In this section its purpose is to explain how a description of the faces of the Voronoi domain $V(0)$ and their duals is provided in our notation for a situation where the results cannot easily be obtained in another way, and how further details of the structure of the faces can be inferred from it if one desires.

3.1. Example A_2

The vertices of $V(0)$ (see figure 1) split into two W-orbits. We provide a representative of each orbit as the following decoration of the A_2 Coxeter–Dynkin diagram.

 $\Longleftrightarrow \omega_1$ and  $\Longleftrightarrow \omega_2$. (3.1)

The full set of $V(0)$ vertices (0-faces) is then obtained by the action of (2.32) of W on the two representatives:

$$\begin{aligned} \omega_1 &: \ r_1\omega_1 = -\omega_1 + \omega_2 \qquad r_2r_1\omega_1 = -\omega_2 \\ \omega_2 &: \ r_2\omega_2 = \ \ \omega_1 - \omega_2 \qquad r_1r_2\omega_2 = -\omega_1. \end{aligned} \tag{3.2}$$

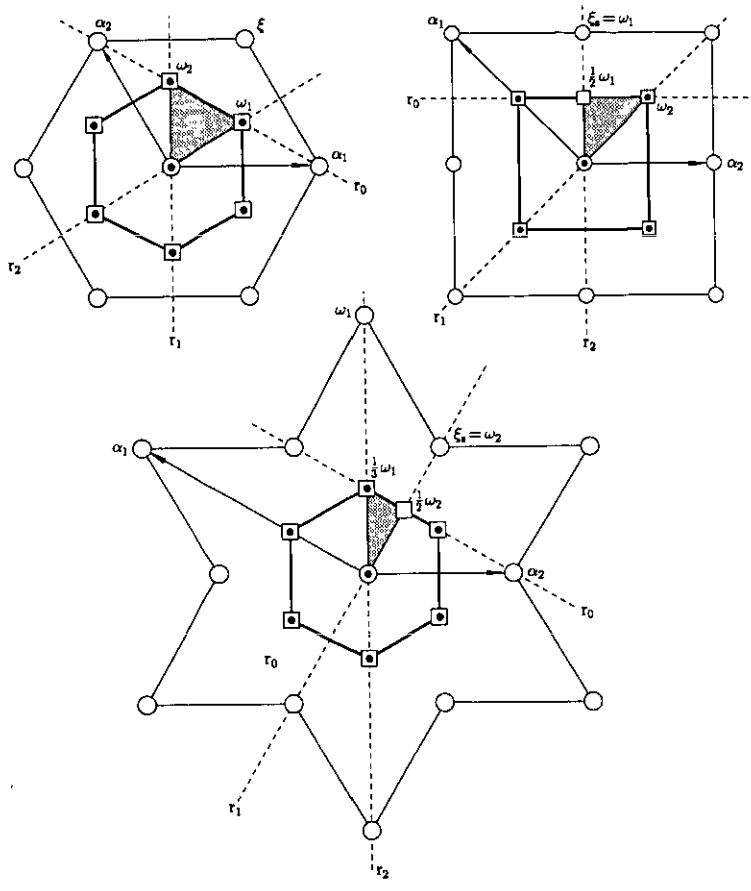

Figure 1. The roots and the Voronoi domains $V(0)$ centred at the origin of the root lattices of the simple Lie groups A_2, B_2, and G_2. The circles denote roots, dotted circle is the origin, dotted boxes are vertices of $V(0)$; α_1 and α_2 are the simple roots; ω_1 and ω_2 are the corresponding fundamental weights; r_0, r_1, and r_2 indicate the broken reflection lines for the action of the generating elements (also denoted r_0, r_1, r_2) of the affine Weyl group; the shaded triangle is the fundamental region; ξ or ξ_s is the highest short root; an open box indicates an auxiliary interior point of a face of $V(0)$ used in our description of the face.

There is only one W-orbit of the edges (1-faces) of $V(0)$. We present it as the decorated diagram

$$\Longleftrightarrow [\omega_1, \omega_2] := \text{ line segment connecting } \omega_1 \text{ and } \omega_2. \tag{3.3}$$

The full set of six 1-faces of $V(0)$ is then obtained by letting the Weyl group act on $[\omega_1, \omega_2]$. More precisely, we find the following distinct 1-faces using (2.32):

$$\begin{aligned}
&[\omega_1, \omega_2] \qquad r_1[\omega_1, \omega_2] = [-\omega_1 + \omega_2, \omega_2] \qquad r_2[\omega_1, \omega_2] = [\omega_1, \omega_1 - \omega_2] \\
&r_2 r_1[\omega_1, \omega_2] = [-\omega_2, \omega_1 - \omega_2] \qquad r_1 r_2[\omega_1, \omega_2] = [-\omega_1 + \omega_2, -\omega_1] \\
&r_1 r_2 r_1[\omega_1, \omega_2] = r_2 r_1 r_2[\omega_1, \omega_2] = [-\omega_2, -\omega_1].
\end{aligned} \tag{3.4}$$

The dual of a face, given by the nearest point of the root lattice to the face, is visible on figure 1. In order to determine the dual of a vertex, say ω_1 (diagram (3.1)), one has to use the reflection r_2, specified by the node ○ of the diagram, and the affine reflection r_0 (see (2.17)) given by the node ⊙, and to apply them to the origin 0. The dual face to ω_1 has as its vertices the images of 0 under the group generated by the two reflections: 0, $r_0 0 = \xi = \alpha_1 + \alpha_2$, and $r_2\xi = \alpha_1$. One finds similarly the dual of ω_2 as the equilateral triangle $[0, r_0 0, r_1 r_0 0] = [0, \xi, \alpha_2]$.

Similarly to get the dual of the edge $[\omega_1, \omega_2]$ we apply the affine reflection r_0 corresponding to ⊙ to the origin obtaining $[0, \xi]$.

3.2. *Example* B_2

The numbering of the nodes of the diagram

stands for indexing the simple roots α_1, α_2, the fundamental weights ω_1, ω_2, and the elementary reflections r_1, r_2.

There is only one W-orbit of vertices of $V(0)$ (see figure1). We provide its representative point ω_2 as the following decoration of the B_2 (equivalently C_2) Coxeter–Dynkin diagram.

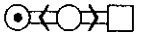 (3.5)

The extension node ⊙ stands for the origin and for the affine reflection r_0 (see (2.17)). This diagram should really be thought of as two subdiagrams

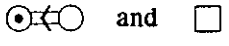 (3.6)

The box stands for ω_2 (it is its position in the B_2 diagram). The full set of four vertices of $V(0)$ consists of

$$\omega_2 \qquad r_2\omega_2 = -\omega_2 + \omega_1 \qquad r_1 r_2 \omega_2 = \omega_2 - \omega_1 \qquad r_2 r_1 r_2 \omega_2 = -\omega_2 \tag{3.7}$$

as follows from (2.32). The dual cell to the vertex ω_2 is described by the complementary piece of the diagram, i.e. the first diagram of (3.6). This stands for the region (square) whose vertices are the translates by the group generated by r_0 and r_1 of ⊙ (i.e. the origin 0):

$$0 \qquad r_0 0 = \xi_s = \alpha_1 + \alpha_2 \qquad r_1 \xi_s = \alpha_2 \qquad r_0 \alpha_2 = \xi = \alpha_1 + 2\alpha_2. \tag{3.8}$$

This is confirmed by looking at figure 1.

The edges of $V(0)$ are represented by the decorated diagram

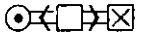 (3.9)

which again may be thought of as

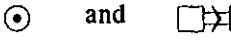 (3.10)

There are several new features here. The two boxes indicate that the edge is being made out of $\omega_1/2$ and ω_2. (The fraction $\frac{1}{2}$ here is important and we will explain

how it can be easily read from the diagram later. However, the boxes stand primarily for ω_1 and ω_2.) The cross indicates that reflection r_2 must be applied to ω_2 to fill out the edge, i.e. the edge is $[\omega_2, r_2\omega_2]$ which contains $\omega_1/2$ as an interior point (actually the midpoint) as one can see on figure 1. The empty box standing for $\omega_1/2$ indicates exactly that $\omega_1/2$ is interior to the edge.

The action of W on the edge $[\omega_2, r_2\omega_2]$ according to (2.32) then provides all the 1-faces of $V(0)$. We have

$$\begin{aligned}
&[\omega_2, r_2\omega_2] = [\omega_2, -\omega_2 + \omega_1] \\
&r_1[\omega_2, r_2\omega_2] = [\omega_2, r_1 r_2\omega_2] = [\omega_2, \omega_2 - \omega_1] \\
&r_2 r_1[\omega_2, r_2\omega_2] = [r_2\omega_2, r_2 r_1 r_2\omega_2] = [-\omega_2 + \omega_1, -\omega_2] \\
&r_1 r_2 r_1[\omega_2, r_2\omega_2] = [r_1 r_2\omega_2, r_2 r_1 r_2\omega_2] = [\omega_2 - \omega_1, -\omega_2]. \qquad (3.11)
\end{aligned}$$

To determine the dual facet to the edge $[\omega_2, r_2\omega_2]$ we turn to the complementary diagram $\odot$. It indicates that we apply the group $\{1, r_0\}$ generated by r_0 to the origin $\odot$ thereby obtaining $[0, r_0 0] = [0, \xi_s]$ as on figure 1.

3.3. Example G_2

We illustrate this example in terms of the algorithm and diagramatic notation that make up our general method.

Beginning with

(3.12)

(the numbers refer to the indexing of the simple roots α_1, α_2 and fundamental weights ω_1, ω_2 and the reflections r_1, r_2), we dualize the graph

(3.13)

and make the standard affine extension

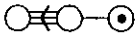

(3.14)

indexing the new node by 0 and indicating it by the special symbol $\odot$.

We next 2-balance this graph [13]. This means assigning positive integer marks $m_i, i = 0, 1, 2$, to the nodes subject to the following conditions:

(i) For each i, $\sum m_j/m_i = 2$, where the sum is over all arrows (with multiplicity) from node j to node i. (Single bonds count as one arrow in each direction, the multiple bonds in (3.14) count as three arrows in one direction and one in the other.)

(ii) $\gcd\{m_0, m_1, m_2\} = 1$.

Thus we have the unique 2-balancing

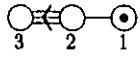

(3.15)

Finally we redualize

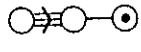

(3.16)

The vertices of the fundamental simplex F which is used in the construction are given as

$$\left\{0, \frac{\omega_1}{m_1}, \frac{\omega_2}{m_2}\right\} = \left\{0, \frac{\omega_1}{3}, \frac{\omega_2}{2}\right\}. \tag{3.17}$$

Our algorithm begins at the maximal dimension facets (faces) which in this case are the edges. We start with

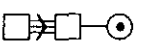 (3.18)

indicating that we use the line segment

$$\left[\frac{\omega_1}{3}, \frac{\omega_2}{2}\right] \tag{3.19}$$

and decorate the diagram to

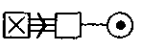 (3.20)

which we should think of as

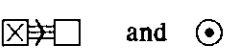 (3.21)

indicating, as in B_2, that the edge is obtained from (3.19) by applying the reflection r_1, and that $\omega_2/2$ is an interior point of the edge. In general, a cross is put in each box that is not adjacent by an edge of the diagram to any node ○ or ⊙. Thus we have the edge

$$\left[\frac{\omega_1}{3}, r_1\frac{\omega_1}{3}\right] = \left[\frac{\omega_1}{3}, -\frac{\omega_1}{3} + \omega_2\right] \tag{3.22}$$

and the remaining edges are determined by the action of the Weyl group elements (reflections) r_1 and r_2 on this edge.

As the dual to the edge (3.22) we have the 1-face determined by the complementary graph which in this case is ⊙. Thus we get the edge

$$[0, r_0 0] = [0, \xi_s] \qquad \text{(see figure 1).}$$

To obtain the vertices of $V(0)$ we replace by ○ in (3.20) any box *not* marked by a cross (equivalently adjacent to a circle node). Here there is only one choice

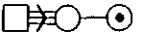 (3.23)

which we think of as

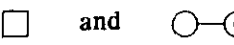 (3.24)

Thus the vertices of $V(0)$ are the W-translates of $\omega_1/3$. The remaining five vertices of $V(0)$ are obtained from $\omega_1/3$ by the action of (2.32) of the Weyl group elements r_1, r_2r_1, $r_1r_2r_1$, $r_2r_1r_2r_1$ and $r_1r_2r_1r_2r_1$ giving respectively $-\frac{1}{3}\omega_1 + \omega_2$, $\frac{2}{3}\omega_1 - \omega_2$, $-\frac{2}{3}\omega_1 + \omega_2$, $\frac{1}{3}\omega_1 - \omega_2$ and $-\frac{1}{3}\omega_3$.

The dual cell to the vertex $\omega_1/3$ is the convex hull (triangle) of the three vertices

$$[0, r_0 0, r_2 r_0 0] = [0, \xi_s, \alpha_1 + \alpha_2].$$

3.4. Example C_4

The Voronoi domain $V(0)$ of the root lattice of the symplectic group C_4 of rank 4 is the same as that of D_4 (the short roots of C_4 form a root system of type D_4). Thus we get the same classification of facets and dual facets from either starting point. There is a similar correspondence for C_3 and $D_3 = A_3$. We do not dwell on this correspondence here since it is pointed out later for general $n \geqslant 4$.

The general method for describing of d-faces and duals for $V(0)$ is given in section 1. The results for all $C_n, n \geqslant 3$, are given in section 5.3, table 6. The particular example of C_4 is used to illustrate the general development of the algorithm in section 4. The reader may wish to see how the classification goes in this case by skimming through section 4 at this point. Our aim here is limited to showing how to extract more information about the facets and their duals once the classification has been carried out (cf table 2).

Table 2. Representative faces of the Voronoi domain $V(0)$ (subdiagram of boxes) of the root lattice C_4, their multiplicities in $V(0)$, and dual faces (subdiagram of circles).

Face	Diagram	#
V(0)	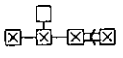	1
3-face	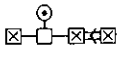	24
2-face	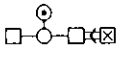	96
1-face	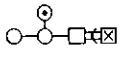	32
1-face	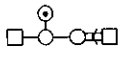	64
0-face	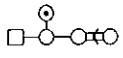	8
0-face	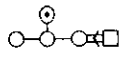	16

There are two classes of vertices of $V(0)$ in the case of C_4

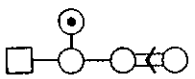 and 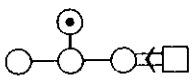 (3.25)

The first diagram gives rise to a W-orbit of eight vertices generated from ω_1:

$$\omega_1 \qquad r_1\omega_1 = -\omega_1 + \omega_2$$

$$r_2r_1\omega_1 = -\omega_2 + \omega_3 \qquad r_3r_2r_1\omega_1 = -\omega_3 + \omega_4$$

$$r_4r_3r_2r_1\omega_1 = \omega_3 - \omega_4 \qquad r_3r_4r_3r_2r_1\omega_1 = \omega_2 - \omega_3$$

$$r_2r_3r_4r_3r_2r_1\omega_1 = \omega_1 - \omega_2 \qquad r_1r_2r_3r_4r_3r_2r_1\omega_1 = -\omega_1. \tag{3.26}$$

Similarly one finds 16 distinct vertices represented by the second decorated diagram for $\frac{1}{2}\omega_4$. These are

$$\begin{aligned} &\pm\tfrac{1}{2}\omega_4 \qquad \pm(\omega_3-\tfrac{1}{2}\omega_4) \qquad \bullet\,(\omega_2-\omega_3+\tfrac{1}{2}\omega_4) \qquad \pm(\omega_2-\tfrac{1}{2}\omega_4)\\ &\pm(\omega_1-\omega_2+\tfrac{1}{2}\omega_4) \qquad \pm(\omega_1-\omega_2-\omega_3-\tfrac{1}{2}\omega_4)\\ &\bullet\,(-\omega_1+\tfrac{1}{2}\omega_4) \qquad \pm(\omega_1-\omega_3+\tfrac{1}{2}\omega_4). \end{aligned} \tag{3.27}$$

The four-dimensional dual cells $D(\omega_1)$ and $D(\frac{1}{2}\omega_4)$ are represented by the sub-diagrams of (3.25)

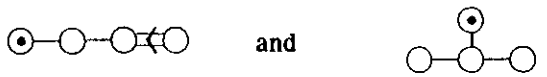 and (3.28)

Each stands for the convex hull of the orbit of the point indicated by the dotted circle (i.e. the origin here) by the group generated by the reflections corresponding to all the circles. This is the well-known Wythoff construction (see section 4.7).

According to [10, 11.7] these diagrams create the four-dimensional crosspolytope (generalized octahedron) and the half-hypercube (obtained by keeping only alternate vertices) respectively (see table 3). Explicitly, the vertices of the crosspolytope $D(\omega_1)$ are the origin 0 and

$$\begin{aligned} &r_0 0 = \xi_s = \omega_2 = \alpha_1 + 2\alpha_2 + 2\alpha_3 + \alpha_4\\ &r_2\omega_2 = \alpha_1 + \alpha_2 + 2\alpha_3 + \alpha_4 = \omega_1 - \omega_2 + \omega_3\\ &r_3 r_2\omega_2 = \alpha_1 + \alpha_2 + \alpha_3 + \alpha_4 = \omega_1 - \omega_3 + \omega_4\\ &r_4 r_3 r_2\omega_2 = \alpha_1 + \alpha_2 + \alpha_3 = \omega_1 + \omega_3 - \omega_4\\ &r_3 r_4 r_3 r_2\omega_2 = \alpha_1 + \alpha_2 = \omega_1 + \omega_2 - \omega_3\\ &r_2 r_3 r_4 r_3 r_2\omega_2 = \alpha_1 = 2\omega_1 - \omega_2\\ &r_0 r_2 r_3 r_4 r_3 r_2\omega_2 = 2\alpha_1 + 2\alpha_2 + 2\alpha_3 + \alpha_4 = 2\omega_1, \end{aligned} \tag{3.29}$$

and for the half hypercube $D(\frac{1}{2}\omega_4)$ the origin 0 together with the following seven vertices

$$\begin{aligned} &r_0 0 = \omega_2 = \alpha_1 + 2\alpha_2 + 2\alpha_3 + \alpha_4\\ &r_2\omega_2 = \alpha_1 + \alpha_2 + 2\alpha_3 + \alpha_4 = \omega_1 - \omega_2 + \omega_3\\ &r_2\omega_2 = \alpha_1 + \alpha_2 + 2\alpha_3 + \alpha_4 = \omega_1 - \omega_2 + \omega_3\\ &r_3 r_2\omega_2 = \alpha_1 + \alpha_2 + 2\alpha_3 + \alpha_4 = \omega_1 - \omega_3 + \omega_4\\ &r_1 r_2\omega_2 = \alpha_2 + 2\alpha_3 + \alpha_4 = -\omega_1 + \omega_3\\ &r_1 r_3 r_2\omega_2 = \alpha_2 + 2\alpha_3 + \alpha_4 = -\omega_1 - \omega_2 - \omega_3 + \omega_4\\ &r_2 r_1 r_3 r_2\omega_2 = \alpha_3 + \alpha_4 = -\omega_2 + \omega_4\\ &r_0 r_1 r_3 r_2\omega_2 = -\omega_1 - \omega_3 + \omega_4. \end{aligned} \tag{3.30}$$

Table 3. Wythoff construction. Diagrams have n nodes with the exception of the last two.

Diagram	Name	Coxeter symbol
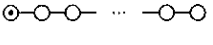	(n+1)-simplex	α_{n+1}
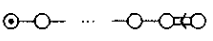	n-cross polytope	β_n
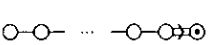	n-cube	γ_n
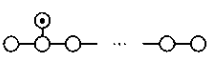	alternate vertices of an n-cube	$h\gamma_n$
	n-cross polytope	β_n
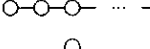	Gosset's 6-dimensional figure	2_{21}
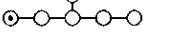	Gosset's 7-dimensional semiregular figure	3_{21}

The 1-faces (edges) of $V(0)$ are classified by the two diagrams

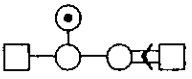 and 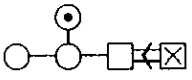 (3.31)

The first gives rise to 64 W-translates of the representative edge $[\omega_1, \frac{1}{2}\omega_4]$. The second diagram represents 32 translates of the edge $[\frac{1}{2}\omega_4, r_4\frac{1}{2}\omega_4] = [\frac{1}{2}\omega_4, \omega_3 - \frac{1}{2}\omega_4]$. Note that the first type of edge has its ends on different W-orbits while the second type has both ends in one orbit.

The dual faces of dimension 3 are regular tetrahedra C, whose vertices are

$$0 \qquad \xi_s \qquad r_2\xi_s \qquad r_3r_2\xi_s \tag{3.32}$$

and

$$0 \qquad \xi_s \qquad r_2\xi_s \qquad r_1r_2\xi_s \tag{3.33}$$

respectively.

There is only one W-orbit of 2-faces.

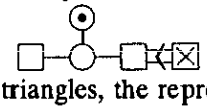 . (3.34)

These are triangles, the representative one being the convex hull of $[\omega_1, \frac{1}{2}\omega_4, r_4\frac{1}{2}\omega_4]$. The dual is the triangle whose vertices are $[0, r_0 0, r_2 r_0 0]$.

Finally there are the 3-faces all represented by the 3-face

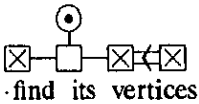 . (3.35)

In order to find its vertices we use the stabilizer of the face, generated by the reflections r_1, r_3, r_4 indicated by the crossed boxes of (3.35), on the representatives of the vertices given in (3.25). These are

$$\omega_1 \qquad r_1\omega_1 = -\omega_1 + \omega_2 \tag{3.36}$$

and

$$\begin{aligned} &\tfrac{1}{2}\omega_4 \\ &r_4\tfrac{1}{2}\omega_4 = \omega_3 - \tfrac{1}{2}\omega_4 \\ &r_3r_4\tfrac{1}{2}\omega_4 = \omega_2 - \omega_3 + \tfrac{1}{2}\omega_4 \\ &r_4r_3r_4\tfrac{1}{2}\omega_4 = \omega_2 - \tfrac{1}{2}\omega_4 \end{aligned} \tag{3.37}$$

of the octahedron. Its dual is the segment $[0, r_0 0] = [0, \xi_3]$.

By continuing further changes in the decoration of the C_4 diagrams, one gets from (3.35), as the next step, the diagram of $V(0)$ shown in table 2. The symmetry group of the diagram, given by the crossed boxes, is now $W(C_4)$. Similarly, we can go one step further in the opposite extreme replacing the single box in (3.25) by ○. The result is the diagram (see table 1) for the root lattice C_4 generated from the origin ⊙ by the reflections r_0, r_1, r_2, r_3, r_4 applied to it.

It remains to explain how one determines the number of faces given by a decorated diagram. It is equal to the size of the corresponding Weyl group orbit which is in turn equal to the ratio of the order of the Weyl group of C_4 to the order of the stabilizer of the open boxes of the decoration. One reads immediately the necessary information from the diagrams:

0-faces:
$$\frac{|W(C_4)|}{|W(C_3)|} = \frac{2^4 \cdot 4!}{2^3 \cdot 3!} = 8 \tag{3.38}$$

$$\frac{|W(C_4)|}{|W(A_3)|} = \frac{2^4 \cdot 4!}{4!} = 16 \tag{3.39}$$

1-faces:
$$\frac{|W(C_4)|}{|W(A_2)|} = \frac{2^4 \cdot 4!}{3!} = 64 \tag{3.40}$$

$$\frac{|W(C_4)|}{|W(A_2)||W(A_1)|} = \frac{2^4 \cdot 4!}{3!2} = 32 \tag{3.41}$$

2-faces:
$$\frac{|W(C_4)|}{|W(A_1)||W(A_1)|} = \frac{2^4 \cdot 4!}{2 \cdot 2} = 96 \tag{3.42}$$

3-faces:
$$\frac{|W(C_4)|}{|W(A_1)||W(C_2)|} = \frac{2^4 \cdot 4!}{2 \cdot 2^2 \cdot 2} = 24. \tag{3.43}$$

All the Weyl group orders are found in table 1.

Similarly we could have established the number of vertices of the four-dimensional dual to the vertices of $V(0)$ prior to the computation (3.29) and (3.30). Regarding the subdiagrams (3.28) of (3.25), we find the size of the W-orbit of ⊙ in each case:

$$\frac{|W(C_4)|}{|W(C_3)|} = \frac{2^4 \cdot 4!}{2^3 \cdot 3!} = 8 \qquad \text{and} \qquad \frac{|W(D_4)|}{|W(A_3)|} = \frac{2^3 \cdot 4!}{4!} = 8. \tag{3.44}$$

As the final part of the example let us ask the following question. Given a vertex, say ω_1, of $V(0)$ of C_4, how many 1-, 2- and 3-faces share that vertex? For that,

we need to apply the stabilizer of ω_1, which is the Weyl group $W(C_3)$ generated by r_2, r_3, r_4, to the representative face containing ω_1 (see section 4.6 for more details). Hence the size of the $W(C_3)$-orbit of the edge $[\omega_1, \frac{1}{2}\omega_4]$ is the ratio of the orders of respective stablizers.

$$\frac{|W(C_3)|}{|W(A_2)|} = \frac{2^3 \cdot 3!}{3!} = 8. \tag{3.45}$$

The second type of 1-face does not contain ω_1 as can be seen in (3.31). Similarly the numbers of 2- and 3-faces containing ω_1 are given by

$$\frac{|W(C_3)|}{|W(A_1 \times A_1)|} = \frac{2^3 \cdot 3!}{2 \cdot 2} = 12, \tag{3.46}$$

$$\frac{|W(C_3)|}{|W(C_2)|} = \frac{2^3 \cdot 3!}{2^2 \cdot 2!} = 6. \tag{3.47}$$

4. General structure of the Voronoi and Delaunay cells

The Voronoi cell $V(0)$ and its facets are determined by certain hyperplanes

$$(x \mid \alpha) = \tfrac{1}{2}(\alpha \mid \alpha) \Longleftrightarrow \langle x, \check{\alpha} \rangle = 1 \tag{4.1}$$

and inequalities

$$(x \mid \beta) < \tfrac{1}{2}(\beta \mid \beta) \Longleftrightarrow \langle x, \check{\beta} \rangle < 1 \tag{4.2}$$

where $\alpha, \beta \in Q \backslash \{0\}$. In particular, we note that any two distinct facets may be distinguished by the sublattice of points of the root lattice that are orthogonal to them.

The convex set $F_0 = \langle \omega_1/m_1, \ldots, \omega_n/m_n \rangle_{\text{conv}}$ is part of some $(n-1)$-face $f = f(n-1)$ of $V(0)$. Since $V(0) = WF$, the boundary of $V(0)$ is the union of the translates of F_0 by W. But F_0 is supported by the hyperplane H_0 of (2.27) and now, using W, we see that the entire boundary of $V(0)$ is contained in the union of hyperplanes

$$\{x \in V \mid \langle x, \check{\alpha} \rangle = 1\}$$

where $\check{\alpha}$ runs through $W\check{\xi}_s = \Delta_s =$ set of short roots of Δ.

This shows that in (4.1) and (4.2) we may restrict ourselves to taking $\alpha, \beta \in \Delta_s$.

Thus each $(n-1)$-face of $V(0)$ orthogonally bisects some line segment $[0, \alpha]$ where $\alpha \in \Delta_s$. This sets up a 1–1 correspondence between $(n-1)$-faces and the set of short roots.

Since for $i = 1, 2, \ldots, n$,

$$\left(\frac{\omega_i}{m_i} \mid \xi_s\right) / (\xi_s \mid \xi_s) = \tfrac{1}{2}\langle \frac{\omega_i}{m_i} \mid \check{\xi}_s \rangle = \tfrac{1}{2} = (\tfrac{1}{2}\xi_s \mid \xi_s) / (\xi_s \mid \xi_s) \tag{4.3}$$

we see that $f(n-1)$ is the $(n-1)$-face corresponding to ξ_s, orthogonal to $[0, \xi_s]$ passing through $\xi_s/2$. The remaining $(n-1)$-faces of $V(0)$ are the W-translates of $f(n-1)$ and are in 1–1 correspondence with the elements of $W/\mathrm{Stab}_W(f)$. But the stabilizer $\mathrm{Stab}_W(f) = \mathrm{Stab}_W(\frac{1}{2}\xi_s)$.

Since ξ_s is the highest short root, ξ_s is dominant and hence lies in the cone of (2.29). As we have seen C is the fundamental region of W and by using (2.20), (iii), we know that $\mathrm{Stab}_W(\xi_s/2)$ is generated by the reflections r_i such that the wall defining it passes through $(\xi_s/2)$:

$$\mathrm{Stab}_W(f) = \langle r_i \mid i = 1, 2, \ldots, n;\ (\alpha_i \mid \xi_s) = 0 \rangle. \tag{4.4}$$

The vertices of $V(0)$ are the W-translates of the vertices of f. The vertices of f are translates by $\mathrm{Stab}_W(f)$ of some of the vertices ω_i/m_i of F. Exactly which ones is part of the problem of describing $V(0)$.

We now explain how we use the 'decorated' Coxeter–Dynkin diagrams to describe the $(n-1)$-faces and all the lower dimensional facets of $V(0)$. We illustrate this as we go along by the example of $V(0)$ of the root lattice of C_4. In this example we thus determine the content of table 2.

Consider the Coxeter–Dynkin diagram of C_4:

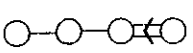

(4.5)

4.1. Determination of the short roots and the marks

Dualize the diagram (4.5) and make the usual affine extension of it. The result is the affine diagram $B_4^{(1)}$.

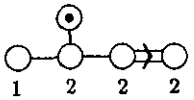

(4.6)

The extension node is shown as ⊙. The marks written on the $B_4^{(1)}$ diagram (4.6) are the coefficients of the highest root of B_4 (i.e. $\check{\xi}_s$ of C_4) and are determined by 2-balancing of the graph [13] (see also example G_2 of section 3).

Redualizing the diagram (4.6) while retaining the marks at the nodes gives us

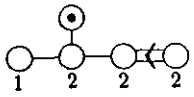

(4.7)

and the fundamental region

$$F(C_4) = \left\langle 0, \frac{\omega_1}{1}, \frac{\omega_2}{2}, \frac{\omega_3}{2}, \frac{\omega_4}{2} \right\rangle_{\mathrm{conv}}$$

of C_4 which lies inside the cone (2.29).

The extension node plays a different role from the others and so is designated ⊙. This becomes clear when we discuss the dual cells. The usual conventions of angles and lengths conveyed by the extended Coxeter–Dynkin diagram are applicable here both to the affine simplex F in which each node corresponds to one reflecting wall of F (⊙ corresponding to H_0) and to the simple roots $\alpha_1, \ldots, \alpha_n$ and the lowest short root $-\xi_s$.

4.2. Determination of the $(n-1)$-faces of $V(0)$

Replace each node ○ (which represents a simple root) by □ which in the jth position of the diagram represents ω_j/m_j. Thus from (4.7) we get

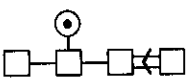

(4.8)

This diagram stands for the $(n-1)$-face $f(n-1)$ determined by

$$\{\omega_1/m_1, \ldots, \omega_n/m_n\}.$$

As we saw, the face f is stabilized by the group generated by the reflections r_i for which $(\alpha_i|\xi_s) = 0$. This information is read directly off the diagram where it is indicated by marking the appropriate boxes:

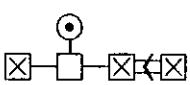

(4.9)

Note that the cross refers to the reflection r_i while □ refers to ω_i/m_i. The number of 3-faces in this example is thus given by the ratio (3.43) of the Weyl group orders.

Obviously the symmetry group G^{n-1} of f in W is $\mathrm{Stab}_W(f)$: in this case

$$G^{n-1} \simeq W(A_1) \times W(B_2). \tag{4.10}$$

We observe that it may happen, as it does here, that only one box, say the ith, is unmarked. In this case the reflections r_j in the $n-1$ marked boxes reflect F_0 in $n-1$ independent directions in V, namely those determined by the corresponding simple roots α_j, while holding ω_i/m_i fixed. Thus the point ω_i/m_i is an *interior* point of the face f (in fact its centre). In particular, ω_i/m_i cannot then be a vertex of $V(0)$.

4.3. The k-facets of $V(0)$

We may now assume that $n > 1$. A k-face $f(k)$ of dimension k of $V(0)$ is determined by a set of equalities and inequalities of the form (4.1) and (4.2), where $\alpha, \beta \in \Delta_s$. Using W we can assume that $f(k) \cap F_0$ supports $f(k)$. Then we may even assume that $\alpha, \beta \in \Delta_s^+$. For

$$x = \sum c_i \frac{\omega_i}{m_i} \qquad \check{\alpha} = \sum d_i \check{\alpha}_i \in \Delta_s^+$$

$$0 \leqslant c_i \leqslant 1 \qquad 0 \leqslant d_j \leqslant m_j \qquad \sum c_i = 1 \tag{4.11}$$

we have

$$\langle x, \check{\alpha} \rangle = \sum \frac{c_i d_i}{m_i}. \tag{4.12}$$

Therefore

$$\langle x, \check{\alpha} \rangle = 1 \iff \sum \frac{c_i d_i}{m_i} = 1 \tag{4.13}$$

which, together with $\sum c_i = 1$, gives

$$\langle x, \check{\alpha} \rangle = 1 \iff \left\langle \frac{\omega_i}{m_i}, \check{\alpha} \right\rangle = 1 \qquad \text{whenever } c_i > 0 \tag{4.14}$$

and hence $f(k) \cap F_0$ is

$$\left\langle \frac{\omega_i}{m_i} \mid \frac{\omega_i}{m_i} \in f(k) \right\rangle_{\text{conv}}. \tag{4.15}$$

(Recall that the facets are closed.) This proves the following lemma.

Lemma 3. For any k-facet $f(k)$ of $V(0)$ whose intersection with F_0 supports it, $f(k) \cap F_0$ is the convex hull of some subset

$$\left\{ \frac{\omega_i}{m_i} \mid i \in S \right\} \qquad S \subset \{1, 2, \ldots, n\}.$$

Continuing with the facet $f = f(k)$, we proceed to determine its dual $f(k)^*$. Set

$$f_0 = \left\langle \frac{\omega_i}{m_i} | i \in S \right\rangle_{\text{conv}} = f(k) \cap F_0. \tag{4.16}$$

Then

$$f^* = f(k)^* = \langle q \in Q \mid f \text{ is a facet of } V(q) \rangle_{\text{conv}}.$$

Of course,

$$V(q) \supset f \iff V(q) \supset f_0.$$

Since the chambers making up $V(0)$ are

$$\{wF \mid w \in W\} = \{wF \mid w \in W_a,\ w0 = 0\}$$

the chambers making up $V(q)$ are

$$\{wF \mid w \in W_a,\ w(0) = q\}.$$

In particular, there is a $w \in W_a$ such that

$$w(0) = q \qquad wF \supset f_0.$$

Then $w^{-1} f_0$ and f_0 are both facets of F. According to (2.20)

(i) w fixes f_0 pointwise;

(ii) w is generated by the reflections in the walls of F which contain f_0.

The walls of F containing f_0 are

$$\left\{ H_{\check{\alpha}_j} \,\middle|\, \left\langle \frac{\omega_i}{m_i}, \check{\alpha}_j \right\rangle = 0,\ i \in S \right\} \qquad H_{\check{\xi}_s, 1} := \{x \in V \mid \langle x, \check{\xi}_s \rangle = 1\}$$

(see (2.17)). Thus w lies in the subgroup

$$W_{a,S} := \langle r_0, r_j \mid j \notin S \rangle. \tag{4.17}$$

Conversely, elements of $W_{a,S}$ clearly pointwise fix f_0, and hence f. Thus

$$f \subset V(q) \iff q \in W_{a,S}(0). \tag{4.18}$$

Lemma 4. The facet $f(k)^*$ dual to $f(k)$ is the convex hull of $W_{a,S}(0)$, where S is given by lemma 3 and $W_{a,S}$ by (4.17).

Lemma 4 describes $f(k)^*$, in terms of the Wythoff construction [5, 10]. See section 4.7 for more details. We are going to see (see the remark later) that

$$S' := \{\check{\xi}_s\} \cup \{\alpha_j \mid j \notin S\} \tag{4.19}$$

is connected (i.e. the subdiagram of the Coxeter–Dynkin diagram corresponding to this set is connected.

Assuming this, we can determine the stabilizer of $f(k)$ in W_a:

$$W_a^f := \mathrm{Stab}_{W_a}(f(k)).$$

Each facet $f(k)$ has a centroid (centre of mass) that is in the relative interior of $f(k)$.

Let c be the centroid of the facet $f(k)$. Then for $w \in W_a$,

$$w \in W_a^f \iff wc = c. \tag{4.20}$$

But

$$f(k) = \bigcup_{w \in W_a^f} w f_0$$

and it follows from (4.20) that $c \in f_0 \subset F$. Thus using (2.21)

$$W_a^f = \langle r_j \mid j = 0, 1, \ldots, n; c \text{ lies in the reflecting hyperplane of } r_j \rangle. \tag{4.21}$$

Furthermore,

$$\begin{aligned} w \in W_a^f &\iff w \text{ stabilizes } f(k)^* \\ &\implies w \text{ stabilizes the real linear span} \end{aligned}$$

$$\langle W_{a,S}(0) \rangle_{\mathbb{R}} = \langle W_{a,S}(\check{\xi}_s) \rangle_{\mathbb{R}} = \sum_{j \notin S} \mathbb{R}\check{\alpha}_j + \mathbb{R}\check{\xi}_s =: L \tag{4.22}$$

by the assumption. Thus $w \in W_a^f$ implies that w stabilizes L. Now W_a^f is generated by the reflections r_j of (4.21) and from (4.22) we have for $j = 1, 2, \ldots, n$,

$$\begin{aligned} r_j \in W_a^f &\implies r_j L = L \\ &\implies \alpha_j \in L \text{ or } \alpha_j \perp L. \end{aligned} \tag{4.23}$$

Thus

$$W_a^f = W_a^1 \times W^2 \tag{4.24}$$

where

$$W_a^1 := \langle r_0, r_j \mid \check{\alpha}_j \in L \rangle \tag{4.25}$$

$$W^2 := \langle r_j \mid \alpha_j \perp L \rangle \tag{4.26}$$

and furthermore

$$W^f := W \cap W_a^f = W^1 \times W^2 \tag{4.27}$$

where

$$W^1 := \langle r_j \mid \check{\alpha}_j \in L \rangle.$$

Suppose that $\operatorname{card} S > 1$ (i.e. $k \geqslant 1$). Then

$$\left(\sum_{j \notin S} \mathbb{R}\check{\alpha}_j \cap \mathbb{R}\check{\xi}_s \right) \cap \Pi = \{\check{\alpha}_j \mid j \notin S\}. \tag{4.28}$$

So we have the neater prescription

$$W_a^1 = \langle r_0, r_i \mid i \notin S \rangle \tag{4.29}$$

$$W^2 = \langle r_i \mid (\alpha_i \mid \alpha_j) = 0 = (\alpha_i \mid \check{\xi}_s), j \notin S \rangle \tag{4.30}$$

$$W^1 = \langle r_i \mid i \notin S \rangle. \tag{4.31}$$

If $\operatorname{card} S = 1$ then $S = \{p\}, f(1) = \{\omega_p/m_p\}$ and $W_a^f = \langle r_0, r_i \mid i \neq p \rangle = W_a^1 \times W^2$ when W_a^1 and W^2 are given again by (4.29) and (4.30). Thus

Lemma 5. Let f be a k-facet supported by its intersection $f_0 := f \cap F_0$ with F_0 given by (4.16). Then

$$\operatorname{Stab}_{W_a}(f) = W_a^1 \times W^2$$

$$\operatorname{Stab}_{W}(f) = W^1 \times W^2$$

where W_a^1, W^2, W^1 are given by (4.29)–(4.31). The pointwise stabilizer $\operatorname{Stab}_W^0(f)$ of f in W is W^1.

4.4. Determination of the $(n-2)$-faces of $V(0)$

Consider now the determination of the $(n-2)$-facets of $V(0)$. Designate such a facet by $f(n-2)$ and assume that $f(n-2) \cap F_0$ supports $f(n-2)$. By lemma 3,

$$f(n-2) \cap F_0 = \left\langle \frac{\omega_1}{m_1}, \ldots, \frac{\widehat{\omega}_p}{m_p}, \ldots, \frac{\omega_n}{m_n} \right\rangle_{\text{conv}} \tag{4.32}$$

indicating that the vertex ω_p/m_p of F_0 is omitted. Note that then $f(n-2) \cap F_0 \subset H_{\alpha_p} \cap H_0$.

However, if box p is marked with a cross, then r_p stabilizes $f = f(n-1)$ and so $H_{\alpha_p} \cap H_0$ passes through the interior of $f(n-1)$ (figure 2). In other words, $H_{\alpha_p} \cap H_0$ cannot support an $(n-2)$-facet of $f(n-1)$ and so ω_p/m_p is not suitable for removal.

Conversely, since $H_{\alpha_j} \cap H_0$ does support a facet of F_0, the only reason that it can fail to support a facet $f(n-2)$ is if it passes through the interior of $f(n-1)$. That means $f(n-1)$ contains points on both sides of H_{α_j}. But we have the general fact that if $x \in F$ then

$$w \in \langle r_i \mid i = 1, \ldots, n;\ i \neq j \rangle \Longrightarrow \langle wx, \check{\alpha}_j \rangle > 0. \tag{4.33}$$

It follows that r_j is involved in 'filling out' $f(n-1)$, i.e. r_j stabilizes $f(n-1)$ and box j is marked with a cross. Thus we have the following lemma.

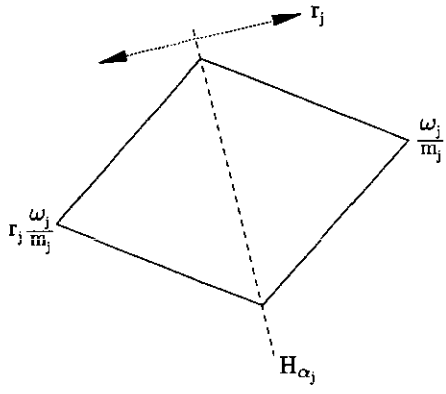

Figure 2. The plane H_{α_j} passing through the interior of a facet.

Lemma 6. $\langle \omega_1/m_1, \ldots, \hat{\omega}_p/m_p, \ldots, \omega_n/m_n \rangle$ supports an $(n-2)$-face iff box p is unmarked.

In our C_4 example, we have only one possibility:

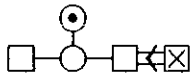

corresponding to

$$\left\langle \frac{\omega_1}{1}, \frac{\omega_3}{2}, \frac{\omega_4}{2} \right\rangle_{\text{conv}}. \tag{4.34}$$

Continuing from lemma 6, since the rest of this $(n-2)$-facet lies in $f(n-1)$, we must determine the subgroup G of $\text{Stab}_w(f)$ that stabilizes $f(n-2)$. Using $S = \{1, \ldots, n\} \backslash \{p\}$ and lemma 5,

$$\text{Stab}_w(f(n-2)) = W^1 \times W^2$$

so that

$$G = \langle r_i \mid i = 1, \ldots, n,\ (\alpha_i \mid \check{\xi}_s) = (\alpha_i \mid \check{\alpha}_p) = 0 \rangle. \tag{4.35}$$

In our example we have the 2-facet given by the diagram (3.34) and again in table 2. Again the information on the stabilizer of the facet has been read directly from the diagram.

4.5. Determination of the $(n-k)$-faces of $V(0)$

We determine $(n-k)$-faces inductively from the $(n-k+1)$- faces. The procedure is precisely the one used earlier to determine the $(n-2)$-faces.

Each $(n-k+1)$-face, call it $f(n-k+1)$, of which there may be more than one orbit under W, is represented at a position where it is supported by a facet of F_0. It is then represented by a decorated Coxeter–Dynkin diagram in which one indicates:

- which ω_i/m_i are used;
- which Weyl subgroup stabilizes it.

The explicit procedure consists of the following:

(i) A subfacet $f(n-k)$ of $f(n-k+1)$ is determined by removal of an ω_i/m_i, the only condition being that this is unmarked by cross.

(ii) The new marking is determined from the old marking by removing the marks from boxes which have edges joining the newly deleted node.

The arguments are trivial modifications of those already used for the $(n-2)$-facets.

In our C_4 example, we thus find the two Weyl group orbits of 1-faces (edges) of $V(0)$ listed in table 2.

Remark. Since the only boxes that may be deleted are those which are not marked and since these are precisely the boxes which are connected to the subdiagram of 'deleted' nodes (i.e. those shown as ○ in the diagram), we see inductively that the subdiagram of deleted nodes is connected. This justifies (4.19). The rule for deleting nodes is precisely equivalent to:

A box may be deleted if and only if it is connected to the subdiagram of previously deleted nodes.

To continue our example, we get the 0-faces of $V(0)$ shown in table 2.

4.6. Inclusions of facets

Let f be a k-face. Let $n > m > k$. We wish to understand the collection of m-faces $\tilde{f}$ such that $\tilde{f} \supset f$. For this purpose we may assume that $f_0 := f \cap F_0$ supports f.

Suppose that $\tilde{f} \supset f$. Then $\tilde{f}$ is some union of W_a-translates of some m-face g of F (actually of F_0) and so there is a $w \in W$ such that $\tilde{f} \supset wg \supset f_0$. Thus some subfacet f_0' of g satisfies $wf_0' = f_0$ and since f_0' and f_0 both lie in F, $f_0' = f_0$ and w pointwise fixes f_0. Thus $w \in \mathrm{Stab}_W(f_0) = \mathrm{Stab}_W^0(f)$, $\tilde{f}' := w^{-1}\tilde{f} \supset g$, and $\tilde{f}' \cap F_0$ supports $\tilde{f}'$. Thus we have the following lemma.

Lemma 7. If $\tilde{f}$ is an m-face containing a k-face f where $f \cap F_0$ supports f, then $\tilde{f}$ is a translate by an element of $\mathrm{Stab}_W^0(f)$ of an m-face $\tilde{f}'$ where $\tilde{f}' \cap F_0$ supports $\tilde{f}'$. The set of m-faces containing f is

$$\mathrm{Stab}_W(f)(\tilde{f}'). \tag{4.36}$$

Suppose that

$$f \cap F_0 = \left\langle \frac{\omega_i}{m_i} | i \in S \right\rangle_{\mathrm{conv}} \qquad \mathrm{card}\, S = k+1. \tag{4.37}$$

Then by lemma 5,

$$\mathrm{Stab}_W^0(f) = W^1 = \langle r_k | k \notin S \rangle. \tag{4.38}$$

Let $\tilde{f}$ be an m-face containing f which, according to lemma 7, we can suppose to satisfy

$$\tilde{f} \cap F_0 = \left\langle \frac{\omega_i}{m_i} | i \in S' \right\rangle_{\mathrm{conv}} \tag{4.39}$$

where $S' \supset S$, $\mathrm{card}\, S' = m + 1$. Then the set of all m-faces containing f in the W-orbit of m-faces generated by $\tilde{f}$ is

$$\mathcal{F}_{\tilde{f},f} := W^1 \tilde{f}. \tag{4.40}$$

We have

$$\mathrm{Stab}_w(\tilde{f}) = \tilde{W}^1 \times \tilde{W}^2$$

$$\tilde{W}^1 := \langle r_k \mid k \notin S' \rangle$$

$$\tilde{W}^2 := \langle r_j \mid (\alpha_i \mid \alpha_j) = 0 = (\tilde{\xi}_s \mid \alpha_j), i \notin S' \rangle.$$

From (4.40)

$$\mathrm{card}\mathcal{F}_{f',f} = [W^1 : W^1 \cap (\tilde{W}^1 \times \tilde{W}^2)]. \tag{4.41}$$

Since for any two subsets $K, L \subset \{1, \ldots, r\}$

$$\langle r_j \mid j \in K \rangle \cap \langle r_j \mid j \in L \rangle = \langle r_j \mid j \in K \cap L \rangle \tag{4.42}$$

it is trivial to compute (4.41). Some examples in the case of C_4 are given at the end of section 3.

4.7. Dual cells

According to lemma 4, if a facet $f(k)$ of $V(0)$ is supported by the set

$$\left\{ \frac{\omega_i}{m_i} \mid i \in S \right\} \tag{4.43}$$

then $f^*(k)$ is the convex hull of

$$W_{a,S}(0) = \langle r_0, r_i \mid i \in S \rangle(0). \tag{4.44}$$

This type of prescription for construction of a polytope is called by Coxeter the Wythoff construction.

The construction is symbolically presented by the Coxeter–Dynkin diagram of the reflection group $W_{a,S}$ with the node for the reflection r_0 specially marked (we use a centre dot $\odot$). This marking indicates that the vertices of $f^*(k)$ all lie on one W-orbit and that the generating point lies on all the reflecting mirrors of the fundamental region except the zeroth, i.e. in this case the point $\odot$ is the origin 0.

Suppose we have given a connected decorated diagram N of (1.1), describing a d-face $f(d)$ by N^d_{Vor} and its $(n-d)$-dimensional dual $f^*(d)$ by N^{n-d}_{Del}.

For example in (3.28) we have N^4_{Del} for either of the two Delaunay cells of the vertices ω_1, and $\frac{1}{2}\omega_4$ of $V(0)$ of the C_4 root lattice, the full diagrams are in (3.25).

We wish to describe the facet structure of the dual $f^*(d)$ of $f(d)$. For this purpose we consider the subgraph N^{n-d}_j of N^{n-d}_{Del},

$$N^{n-d}_j \qquad 0 \leqslant j < n-d \tag{4.45}$$

where N_j^{n-d} is connected, contains $\odot$, and a total j nodes. It represents a W-orbit of j-dimensional subfaces of $f^*(d)$.

In our example the dual cell to the vertex $\frac{1}{2}\omega_4$ is given by lemma 4 as the second diagram of (3.28). In table 2 we supply the identification of these polytopes as provided in [10, section 11.7] and [5, ch 21]. In this example let us describe the facets of the half-hypercube of each type. The admissible subgraphs of the diagram, indicated by open boxes, are the following

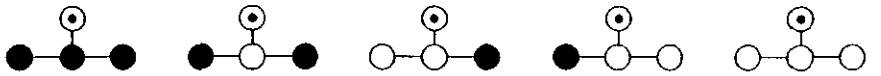

(4.46)

In the present case we are considering the convex hull of the origin 0 by the group

$$W_4 = \langle r_0, r_1, r_2, r_3 \rangle \simeq W(D_4).$$

The stabilizer of 0 is generated by the reflections of W_4 whose hyperplanes pass through 0:

$$\langle r_1, r_2, r_3 \rangle \simeq W(A_3). \tag{4.47}$$

The number of vertices of the half-hypercube is

$$\frac{|\, W(D_4)\,|}{|\, W(A_3)\,|} = 8. \tag{4.48}$$

The edges are the $W(D_4)$-orbit of the representative edge $[0, r_0 0] = [0, \xi_s]$. Its stabilizer is generated by r_0 and those reflections r_i of W_4 whose hyperplane passes through the edge; i.e. precisely those which are orthogonal to the hyperplane for r_0:

$$\langle r_0, r_1, r_3 \rangle \simeq W(A_1 \times A_1 \times A_1).$$

The number of edges of the half-hypercube is

$$\frac{|\, W(D_4)}{|\, W(A_1 \times A_1 \times A_1)\,|} = 24. \tag{4.49}$$

Similarly the 2-faces are $W(D_4)$-orbits of $[0, r_0 0, r_2 r_0 0]$ and whose stabilizer is generated by $\langle r_0, r_2 \rangle \simeq W(A_2)$ and those reflections r_i of $W(D_4)$ (in this case none) whose hyperplanes contain the face.

The number of 2-faces is

$$\frac{W(D_4)\,|}{|\, W(A_2)\,|} = 32. \tag{4.50}$$

The 3-faces are of two kinds (relative to W_4):

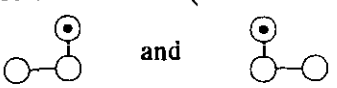

These are 3-simplexes and give rise to

$$\frac{|\, W(D_4)\,|}{|\, W(A_3)\,|} = 8 \tag{4.51}$$

3-faces of each type. Similarly for the other set of holes

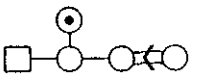

(4.52)

we have the four-dimensional cross-polytape (β_4) with the following numbers of

Vertices: $$\frac{|W(C_4)|}{|W(C_3)|} = 8 \tag{4.53}$$

Edges: $$\frac{|W(C_4)|}{|W(A_1) \times W(C_2)|} = 24 \tag{4.54}$$

2-faces: $$\frac{|W(C_4)|}{|W(A_2) \times W(A_1)|} = 32 \tag{4.55}$$

3-faces: $$\frac{|W(C_4)|}{|W(A_3)|} = 16. \tag{4.56}$$

In this example it happens that β_4 and $h\gamma_4$ are the same, although we note that the group of symmetries in the second case is twice as large and is able to fuse the two orbits of 3-faces. For $C_n, n \geqslant 5$, the duals of the two types of holes are genuinely different. For an alternative proof of the results of section 4 see [12].

5. Classification of Voronoi and Delaunay domains

In this section we present the results of an application of our method described in section 4 to the root lattices of types $A_n (n \geqslant 1)$, B_n $(n \geqslant 2)$, C_n $(n \geqslant 3)$, D_n $(n \geqslant 4)$, E_6, E_7, E_8, F_4, and G_2.

5.1. The root lattice A_n

An application of the method described in section 4 to the d-faces of $V(0)$ of the root lattice $A_n, n \geqslant 1$, yields the results summarized in table 4.

In this case

$$\xi = \xi_s = \alpha_1 + \alpha_2 + \cdots + \alpha_n = \omega_1 + \omega_n$$

and consequently all the marks m_i are the same, $m_i = 1$ for $1 \leqslant i \leqslant n$. The boxes of a decorated Coxeter–Dynkin diagram stand for the corresponding fundamental weights.

In general, there are $n - d$ different types of d-faces of $V(0)$, each type is represented by one decoration shown in table 4.

The n different types of 0-faces (vertices) are represented by the fundamental weights ω_j, $j = 1, 2, \ldots, n$. The number of vertices of type ω_j is equal to the size of W-orbit containing ω_j, namely

$$\frac{|W(A_n)|}{|W(A_{n-j})||W(A_{j-1})|} = \frac{(n+1)!}{(n-j+1)!\,j!} = \binom{n+1}{j}. \tag{5.1}$$

Table 4. The representative faces of $V(0)$ of the root lattice A_n, $n \geqslant 2$, and their duals.

Face dimension	Diagram	Number of faces
n-1	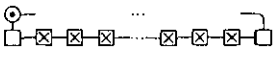	$(n+1)n$
n-2	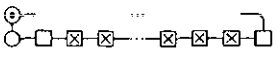	$(n+1)\binom{n}{2}$
n-2	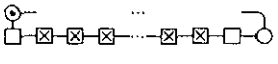	$(n+1)\binom{n}{2}$
d	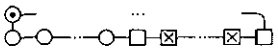	
d	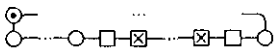	
d	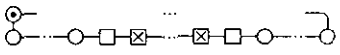	$\binom{n+1}{d+k+1}\binom{d+k+1}{d}$ $0\leq d\leq n-1,\ 0\leq k\leq n-d-1$
d	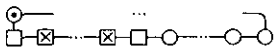	
2	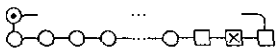	
2	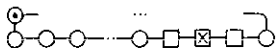	
2	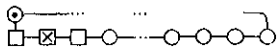	
1	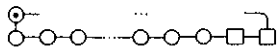	
1	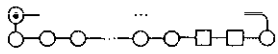	
1	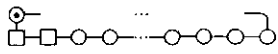	
0	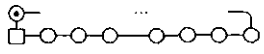	
0	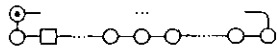	
0	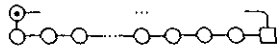	

Consequently, the total number N_0 of 0-faces of $V(0)$ of A_n is given by

$$N_0 = \sum_{j=1}^{n} \binom{n+1}{j} = \sum_{j=0}^{n+1} \binom{n+1}{j} - 2 = 2^{n+1} - 2. \tag{5.2}$$

A generic d-face is given by the diagram

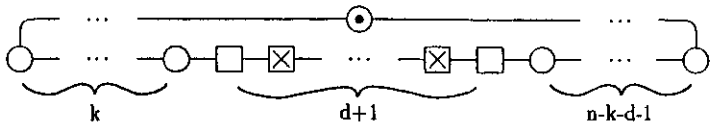

(5.3)

where $0 \leqslant k \leqslant n-d-1$ and $0 \leqslant d \leqslant n-1$, $n \geqslant 1$. The number of faces of this type is given by

$$\frac{|W(A_n)|}{|W(A_k)||W(A_{d-1})||W(A_{n-k-d-1})|} = \frac{(n+1)!}{(k+1)!\,d!\,(n-k-d)!}. \tag{5.4}$$

The total number N_d of d-faces of all types is thus

$$N_d = \sum_{k=0}^{n-d-1} \frac{(n+1)!}{(k+1)!\,d!\,(n-k-d)!} = \binom{n+1}{d}(2^{n+1-d}-2). \tag{5.5}$$

Finally let us verify the validity of the Euler formula (2.33) for A_n. Substituting (5.5) for N_d in (2.33), we have the identity

$$1-(-1)^n = \sum_{d=0}^{n-1}(-1)^d \binom{n+1}{d}(2^{n+1-d}-2). \tag{5.6}$$

The properties of Delaunay domains of A_n and their faces are similarly read from the table 4. For every vertex ω_k of $V(0)$ we have its dual $D(\omega_k)$ of dimension n. The subdiagram of circle nodes of the diagram of ω_k has the structure

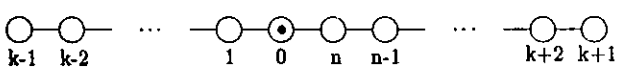

(5.7)

(here we are showing the numbering of the nodes). The kth node is the box which was deleted. The symmetry group in W_a of $D(\omega_k)$ is $W(A_n)$ generated by the reflections indicated by the nodes of (5.7). The number of vertices of $D(\omega_k)$ is the size of the $W(A_n)$-orbit of the node $\odot$:

$$\frac{|W(A_n)|}{|W(A_{k-1})||W(A_{n-k})|} = \frac{(n+1)!}{k!(n-k+1)!} = \binom{n+1}{k}. \tag{5.8}$$

According to section 4.7. the edges of $D(\omega_k)$ are $W(A_n)$ conjugates of the one containing $\odot$, namely $[0, r_0 0]$. Its stabilizer is $W(A_{k-2} \times A_1 \times A_{n-k-1})$. Hence $D(\omega_k), k \geqslant 2$, has the following number of edges:

$$\frac{(n+1)!}{(k-1)!(n-k)!2}. \tag{5.9}$$

Even for $D(\omega_1)$ we find that (5.9) with $k=1$ gives the correct number of edges, namely $\binom{n+1}{2}$.

Table 5. The representative faces of $V(0)$ of the root lattice B_n, $n \geqslant 2$, and their duals.

Face dimension	Diagram	Number of faces
n-1	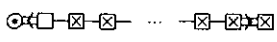	2n
n-2	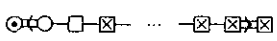	2n(n-1)
d	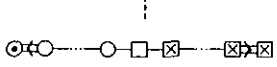	$2^{n-d}d\binom{n}{d}$
2	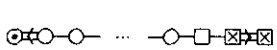	$2^{n-2}\binom{n}{2}$
1	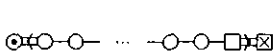	$2^{n-1}n$
0	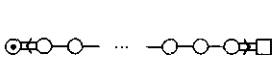	2^n

5.2. The root lattice B_n

The method of section 4, applied to the $B_n, n \geqslant 3$, case gives the diagrams summarized in table 5.

The highest short root of B_n is

$$\xi_s = \alpha_1 + \alpha_2 + \cdots + \alpha_n = \omega_n. \tag{5.10}$$

The marks m_i are found from the dual Coxeter–Dynkin diagram to B_n which is the C_n diagram, $\check{\alpha}_n$ being its long simple root. The highest long root of C_n is

$$\check{\xi}_s = \sum_{i=1}^{n} m_i \check{\alpha}_1 = 2\check{\alpha}_1 + \cdots + 2\check{\alpha}_{n-1} + \check{\alpha}_n. \tag{5.11}$$

Hence the boxes of the decorated diagram stand for

$$\frac{\omega_1}{2}, \frac{\omega_2}{2}, \ldots, \frac{\omega_{n-1}}{2}, \frac{\omega_n}{1}. \tag{5.12}$$

The Voronoi cell $V(0)$ is a hypercube. All d-faces are of one type. Their number N_d is given by

$$N_d = \frac{|W(B_n)|}{|W(A_{n-d-1})||W(B_d)|} = \frac{2^n n!}{(n-d)!\,2^d\,d!} = 2^{n-d}\binom{n}{d}. \tag{5.13}$$

The Euler formula (2.33) in this case is easily verified using (5.13):

$$\sum_{d=0}^{n-1}(-1)^d N_d = \sum_{d=0}^{n-1}(-1)^d 2^{n-d}\binom{n}{d} = 1 - (-1)^n. \tag{5.14}$$

Table 6. The representative faces of $V(0)$ of the root lattice C_n, $n \geqslant 3$, and their duals.

Face dimension	Diagram	Number of faces
n-1	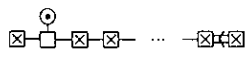	$2^2\binom{n}{n-2}$
n-2	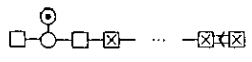	$2^3(n-2)\binom{n}{n-2}$
n-3	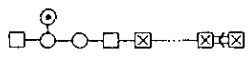	$2^4(n-3)\binom{n}{n-3}$
n-3	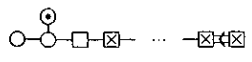	$2^3\binom{n}{n-3}$
	⋮	
d	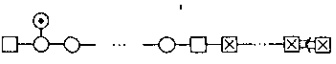	$2^{n-d-1}d\binom{n}{d}$
d	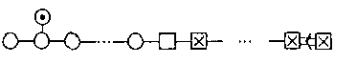	$2^{n-d}\binom{n}{d}$
	⋮	
2	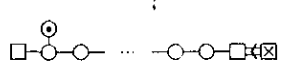	$2^n\binom{n}{2}$
2	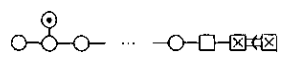	$2^{n-2}\binom{n}{2}$
1	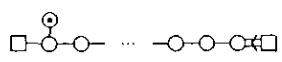	$2^n n$
1	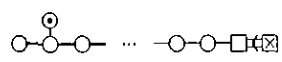	$2^{n-1}n$
0	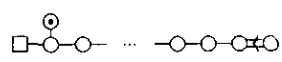	$2n$
0	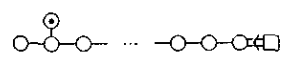	2^n

The Delaunay domain $D(\omega_n)$ of the B_n root lattice is also a hypercube. Its symmetry group in W_a is $W(B_n)$ generated by $r_p, 0 \leqslant p \leqslant n-1$. It has

$$\frac{|W(B_n)|}{|W(A_{n-1})|} = 2^n \tag{5.15}$$

vertices represented by 0,

$$\frac{|W(B_n)|}{|W(A_{n-2})| \cdot |W(A_1)|} = 2^{n-1}n \tag{5.16}$$

edges represented by $[0, r_0 0]$,

$$\frac{|W(B_n)|}{|W(A_{n-3})| \cdot |W(B_2)|} = \frac{2^n n!}{(n-2)!2^3} \tag{5.17}$$

2-faces represented by the triangle $[0, r_0 0, r_1 r_0 0]$, etc.

5.3. The root lattice C_n

The application of our method to C_n, $n \geqslant 2$, gives the results summarized in table 6.

The highest short root ξ_s is

$$\xi_s = \alpha_1 + 2\alpha_2 + 2\alpha_3 + \cdots + 2\alpha_{n-1} + \alpha_n = \omega_2 \tag{5.18}$$

and

$$\check{\xi}_s = \check{\alpha}_1 + 2\check{\alpha}_2 + 2\check{\alpha}_3 + \cdots + 2\check{\alpha}_n . \tag{5.19}$$

Therefore the boxes of the decorated Coxeter–Dynkin diagram denote the points

$$\frac{\omega_1}{1}, \frac{\omega_2}{2}, \frac{\omega_3}{2}, \ldots, \frac{\omega_n}{2}. \tag{5.20}$$

The fundamental region F given by its vertices is thus

$$F = \left\langle 0, \frac{\omega_1}{1}, \frac{\omega_2}{2}, \frac{\omega_3}{2}, \ldots, \frac{\omega_n}{2} \right\rangle . \tag{5.21}$$

Among those only ω_1 and $\omega_n/2$ are the vertices of $V(0)$.

The Voronoi domains of C_n have one type of face of dimensions $d = n-1$ and $n-2$, and two types of face for $0 \leqslant d \leqslant n-3$.

In order to determine N_d for $0 \leqslant d \leqslant n-3$, we have to add up contributions from the two types of face, treating the case $d = 0$ separately:

$$N_0 = \frac{|W(C_n)|}{|W(A_{n-1})|} + \frac{|W(C_n)|}{|W(C_{n-1})|} = \frac{2^n n!}{n!} + \frac{2^n n!}{2^n (n-1)!} = 2^n + 2n. \tag{5.22}$$

$$N_d = \frac{|W(C_n)|}{|W(A_{n-d-1})||W(C_d)|} + \frac{|W(C_n)|}{|W(A_{n-d-1})||W(C_{d-1})|}$$

$$= 2^{n-d}\binom{n}{d} + 2^{n-d+1} d \binom{n}{d} \qquad 1 \leqslant d \leqslant n-3. \tag{5.23}$$

The numbers N_{n-2} and N_{n-1} are found as follows:

$$N_{n-2} = \frac{|W(C_n)|}{|W(A_1)||W(C_{n-3})|} = \frac{2^n n!}{2 \cdot 2^{n-3}(n-3)!} = 2^3 (n-2)\binom{n}{n-2} \tag{5.24}$$

$$N_{n-1} = \frac{|W(C_n)|}{|W(A_1)||W(C_{n-2})|} = 2^2 \binom{n}{n-2}. \tag{5.25}$$

Finally let us verify the validity of the Euler formula in the present case. For that we substitute (5.22)–(5.25) into (2.33). We have

$$\sum_{d=0}^{n-1} (-1)^d N_d$$

$$= 2^n + 2n + \sum_{d=1}^{n-3} (-1)^d 2^{n-d} \binom{n}{d} + \sum_{d=1}^{n-3} (-1)^d 2^{n-d+1} d \binom{n}{d}$$

$$+ (-1)^{n-2} 2^3 (n-2)\binom{n}{n-2} + (-1)^{n-1} 2^2 \binom{n}{n-2}$$

$$= 1 - (-1)^n. \tag{5.26}$$

There are two types of Delaunay domains of $V(0)$ of C_n root lattice: $D(\omega_n/2)$ and $D(\omega_1)$. These are the half-cube $h\gamma_n$ and the cross polytope β_n respectively (see table 3). Their symmetry groups in W_a are respectively

$$W(D_n) = \langle r_0, r_1, r_2, \ldots, r_{n-1} \rangle$$
$$W(C_n) = \langle r_0, r_2, r_3, \ldots, r_n \rangle. \tag{5.27}$$

They have

$$\frac{|W(D_n)|}{|W(A_{n-1})|} = 2^{n-1} \qquad \text{and} \qquad \frac{|W(C_n)|}{|W(C_{n-1})|} = 2n \tag{5.28}$$

vertices (cf (3.30) and (3.29)),

$$\frac{|W(D_n)|}{|W(A_1 \times A_1 \times A_{n-3})|} = 2^{n-2}\binom{n}{2} \qquad \text{and} \qquad \frac{|W(C_n)|}{|W(C_{n-2})||W(A_1)|} = 2^2\binom{n}{2} \tag{5.29}$$

edges, etc.

5.4. The root lattice D_n

The results of our computation of faces of $V(0)$ for D_n, $n \geqslant 4$, are shown in table 7.

In the present case we have

$$\xi = \xi_s = \check{\xi}_s = \omega_2 = \alpha_1 + 2\alpha_2 + 2\alpha_3 + \cdots + 2\alpha_{n-2} + \alpha_{n-1} + \alpha_n. \tag{5.30}$$

Hence the boxes of the decorated diagram denote the points

$$\frac{\omega_1}{1}, \frac{\omega_2}{2}, \frac{\omega_3}{2}, \ldots, \frac{\omega_{n-2}}{2}, \frac{\omega_{n-1}}{1}, \frac{\omega_n}{1} \tag{5.31}$$

and the fundamental region F is given by its vertices as

$$F = \left\langle 0, \frac{\omega_1}{1}, \frac{\omega_2}{2}, \frac{\omega_3}{2}, \ldots, \frac{\omega_{n-2}}{2}, \frac{\omega_{n-1}}{1}, \frac{\omega_n}{1} \right\rangle. \tag{5.32}$$

Among these only ω_1, ω_{n-1} and ω_n are also vertices of $V(0)$, representing the three Weyl group orbits of vertices of $V(0)$.

The Voronoi domains of the D_n root lattice have one type of face for dimensions $n-1$ and $n-2$, two types of face for dimensions $2 \leqslant d \leqslant n-3$, and three types of face of dimensions $d = 1$ and 0.

The total number of vertices of $V(0)$ is given by

$$N_0 = \frac{|W(D_n)|}{|W(D_{n-1})|} + 2\frac{|W(D_n)|}{|W(A_{n-1})|} = \frac{2^{n-1}n!}{2^{n-2}(n-1)!} + 2\frac{2^{n-1}n!}{n!} \tag{5.33}$$
$$= 2n + 2^n.$$

The 1-faces of $V(0)$, given by their vertices, are the following three

$$[\omega_1, \omega_{n-1}] \qquad [\omega_1, \omega_n] \qquad [\omega_{n-1}, \omega_n]. \tag{5.34}$$

Table 7. The representative faces of $V(0)$ of the root lattice D_n, $n \geqslant 4$, and their duals.

Face dimension	Diagram	Number of faces
n-1	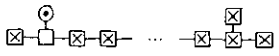	$2^2\binom{n}{n-2}$
n-2	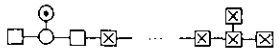	$2^3(n-2)\binom{n}{n-2}$
n-3	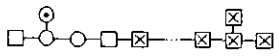	$2^4(n-3)\binom{n}{n-3}$
n-3	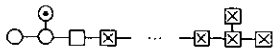	$2^3\binom{n}{n-3}$
	⋮	
d	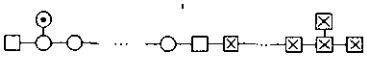	$2^{n-d-1}d\binom{n}{d}$
d	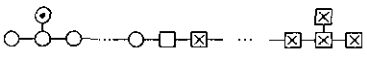	$2^{n-d}\binom{n}{d}$
	⋮	
3	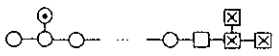	$2^{n-3}\binom{n}{3}$
3	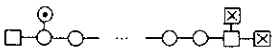	$2^{n-2}3\binom{n}{3}$
2	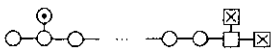	$2^{n-2}\binom{n}{2}$
2	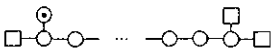	$2^n\binom{n}{2}$
1	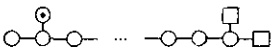	$2^{n-1}n$
1	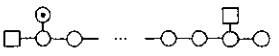	$2^{n-1}n$
1	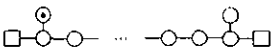	$2^{n-1}n$
0	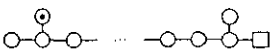	2^{n-1}
0	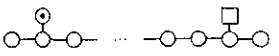	2^{n-1}
0	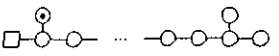	$2n$

Their numbers in $V(0)$ are equal because their stabilizers are isomorphic to $W(A_{n-2})$. One has

$$N_1 = 3\frac{|W(D_n)|}{|W(A_{n-2})|} = 3\frac{2^{n-1}n!}{(n-1)!} = 3\cdot 2^{n-1}n. \tag{5.35}$$

For $2 \leqslant d \leqslant n-3$ the number of d-faces N_d is a sum of two terms

$$\begin{aligned} N_d &= \frac{|W(D_n)|}{|W(A_{n-d-1})||W(D_{d-1})|} + \frac{|W(D_n)|}{|W(A_{n-d-1})||W(D_d)|} \\ &= \frac{2^{n-1}n!}{(n-d)!2^{d-2}(d-1)!} + \frac{2^{n-1}n!}{(n-d)!2^{d-1}d!} \\ &= 2^{n-d+1}d\binom{n}{d} + 2^{n-d}\binom{n}{d}. \end{aligned} \tag{5.36}$$

Finally for N_{n-1} and N_{n-2} we have

$$N_{n-2} = \frac{|W(D_n)|}{|W(A_1)||W(D_{n-3})|} = \frac{2^{n-1}n!}{2\cdot 2^{n-4}(n-3)!} = 2^3(n-2)\binom{n}{n-2}$$

$$N_{n-1} = \frac{|W(D_n)|}{|W(A_1)||W(D_{n-2})|} = \frac{2^{n-1}n!}{2\cdot 2^{n-3}(n-2)!} = 2^2\binom{n}{n-2}. \tag{5.37}$$

Since the short roots of C_n form a root system of type D_n, the root lattices of types C_n and D_n are equal. It is therefore no surprise that the numbers N_d coincide.

There are three orbits of Delaunay domains in $V(0)$ of $D_n (n \geqslant 4)$: $D(\omega_1)$, $D(\omega_{n-1})$, $D(\omega_n)$. Two are half-cubes $h\gamma_n$ and one is the cross polytope β_n. Viewed in C_n the two orbits of half-cubes are fused into one orbit, as we have seen.

5.5. The root lattice E_6

Our results concerning the faces of $V(0)$ of E_6 are found in table 8.

In this case

$$\xi = \xi_s = \check{\xi}_s = \alpha_1 + 2\alpha_2 + 3\alpha_3 + 2\alpha_4 + \alpha_5 + 2\alpha_6 = \omega_6. \tag{5.38}$$

The boxes of the Coxeter–Dynkin diagram decoration therefore stand for the points

$$\frac{\omega_1}{1}, \frac{\omega_2}{2}, \frac{\omega_3}{3}, \frac{\omega_4}{2}, \frac{\omega_5}{1}, \frac{\omega_6}{2}. \tag{5.39}$$

The vertices of the fundamental region are

$$F = \left\langle 0, \frac{\omega_1}{1}, \frac{\omega_2}{2}, \frac{\omega_3}{3}, \frac{\omega_4}{2}, \frac{\omega_5}{1}, \frac{\omega_6}{2} \right\rangle. \tag{5.40}$$

Among them ω_1 and ω_5 are also vertices of $V(0)$.

The Euler formula is readily verified. Indeed, one has from table 8

$$N_0 + N_2 + N_4 = N_1 + N_3 + N_5 = 2934. \tag{5.41}$$

The Delaunay domains $D(\omega_1)$ and $D(\omega_5)$ of $V(0)$ differ by the automorphism of the diagram. They are copies of Gosset's polytope 2_{21}. We consider only one of

Table 8. The representative faces of $V(0)$ of the root lattice E_6 and their duals.

Face dimension	Diagram	Number of faces
5	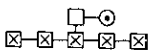	$2^3\,3^2$
4	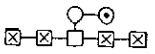	$2^4\,3^2\,5$
3	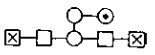	$2^4\,3^3\,5$
2	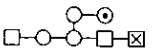	$2^3\,3^3\,5$
2	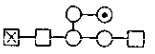	$2^3\,3^3\,5$
1	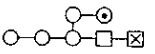	$2^3\,3^3$
1	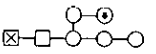	$2^3\,3^3$
1	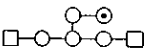	$2\,3^3\,5$
0	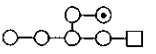	3^3
0	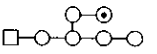	2^3

them. The symmetry group in W_a is $W(D(\omega_1)) = W(E_6)$, and

$$
\begin{aligned}
N_0 &= \frac{|W(E_6)|}{|W(D_5)|} = 3^3 \\
N_1 &= \frac{|W(E_6)|}{|W(A_1 \times A_4)|} = 2^3 \cdot 3^3 \\
N_2 &= \frac{|W(E_6)|}{|W(A_2 \times A_2 \times A_1)|} = 2^4 \cdot 3^2 \cdot 5 \\
N_3 &= \frac{|W(E_6)|}{|W(A_3 \times A_1)|} = 2^3 \cdot 3^3 \cdot 5 \\
N_4 &= \frac{|W(E_6)|}{|W(A_4 \times A_1)|} + \frac{|W(E_6)|}{|W(A_4)|} = 2^3 \cdot 3^4 \\
N_5 &= \frac{|W(E_6)|}{|W(D_5)|} + \frac{|W(E_6)|}{|W(A_5)|} = 3^2 \cdot 11
\end{aligned}
\tag{5.42}
$$

verifying (2.33): $N_0 + N_2 + N_4 = N_1 + N_3 + N_5$.

5.6. The root lattice E_7

Table 9 contains the representative faces and the number of times they occur.

For E_7 we have

$$\xi = \xi_s = \check{\xi}_s = 2\alpha_1 + 3\alpha_2 + 4\alpha_3 + 3\alpha_4 + 2\alpha_5 + \alpha_6 + 2\alpha_7 = \omega_1. \tag{5.43}$$

Thus the boxes of the diagram indicate the points

$$\frac{\omega_1}{2}, \frac{\omega_2}{3}, \frac{\omega_3}{4}, \frac{\omega_4}{3}, \frac{\omega_5}{2}, \frac{\omega_6}{1}, \frac{\omega_7}{2} \tag{5.44}$$

and

$$F = \left\langle 0, \frac{\omega_1}{2}, \frac{\omega_2}{3}, \frac{\omega_3}{4}, \frac{\omega_4}{3}, \frac{\omega_5}{2}, \frac{\omega_6}{1}, \frac{\omega_7}{2} \right\rangle. \tag{5.45}$$

The $V(0)$ vertices split into two W-orbits represented by ω_6 and $\omega_7/2$.

The Euler formula is verified directly using N_d of table 9:

$$N_0 + N_2 + N_4 + N_6 = N_1 + N_3 + N_5 + 2 = 26966. \tag{5.46}$$

The two Delaunay cells of $V(0)$, $D(\omega_6)$ and $D(\omega_7/2)$ are very different. $D(\omega_6)$ is Gosset's polytope 3_{21} and $D(\omega_7/2)$ is an 8-simplex. Their symmetry groups are $W(E_7)$ and $W(A_7)$ respectively. Consequently, we find

$$\begin{aligned} N_0(D(\omega_6)) &= \frac{|W(E_7)|}{|W(E_6)|} = 2^3 \cdot 7 \\ N_0(D(\omega_7/2)) &= \frac{|W(A_7)|}{|W(A_6)|} = 2^3 \\ N_1(D(\omega_6)) &= \frac{|W(E_7)|}{|W(A_1 \times D_5)|} = 2^2 \cdot 3^3 \cdot 7 \\ N_1(D(\omega_7/2)) &= \frac{|W(A_7)|}{|W(A_1 \times A_5)|} = 2^2 \cdot 7 \end{aligned} \tag{5.47}$$

etc.

5.7. The root lattice E_8

Table 10 contains our description of $V(0)$ faces of all dimensions and their multiplicities.

For E_8 we have

$$\xi = \xi_s = \check{\xi}_s = 2\alpha_1 + 3\alpha_2 + 4\alpha_3 + 5\alpha_4 + 6\alpha_5 + 4\alpha_6 + 2\alpha_7 + 3\alpha_8 = \omega_1. \tag{5.48}$$

Therefore the boxes of the diagram stand for the points

$$\frac{\omega_1}{2}, \frac{\omega_2}{3}, \frac{\omega_3}{4}, \frac{\omega_4}{5}, \frac{\omega_5}{6}, \frac{\omega_6}{4}, \frac{\omega_7}{2}, \frac{\omega_8}{3} \tag{5.49}$$

and they together with the origin are the vertices of F.

Checking Euler's formula by the entries N_d of table 10 gives the following

$$N_0 + N_2 + N_4 + N_6 = N_1 + N_3 + N_5 + N_7 = 751920. \tag{5.50}$$

Table 9. The representative faces of $V(0)$ of the root lattice E_7 and their duals.

Face dimension	Diagram	Number of faces
6	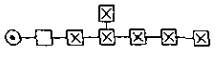	$2\,3^2\,7$
5	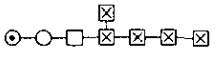	$2^5\,3^2\,7$
4	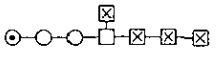	$2^5\,3^2\,5\,7$
3	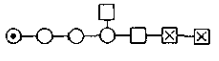	$2^6\,3^2\,5\,7$
2	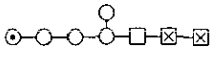	$2^6\,3^2\,7$
2	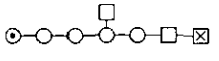	$2^6\,3^2\,7$
1	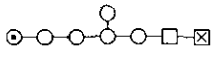	$2^2\,3^3\,7$
1	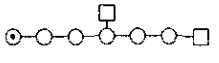	$2^6\,3^2\,7$
0	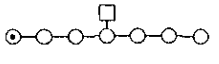	$2^6\,3^2$
0	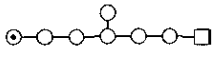	$2^9\,7$

The Delaunay domains $D(\omega_7/2)$ and $D(\omega_8/3)$ of $V(0)$ of E_8 are the 8-cross polytope and the 9-simplex respectively with the symmetry groups $W(D_8)$ and $W(A_8)$. Consequently, we find the following numbers of d-faces of $D(\omega_7/2)$.

$$N_0 = \frac{|W(D_8)|}{|W(D_7)|} = 16 \qquad N_1 = \frac{|W(D_8)|}{|W(A_1 \times D_6)|} = 112$$

$$N_2 = \frac{|W(D_8)|}{|W(A_2 \times D_5)|} = 448 \qquad N_3 = \frac{|W(D_8)|}{|W(A_3 \times D_4)|} = 1120$$

$$N_4 = \frac{|W(D_8)|}{|W(A_4 \times A_3)|} = 896 \qquad N_5 = \frac{|W(D_8)|}{|W(A_5 \times A_1 \times A_1)|} = 896$$

$$N_6 = \frac{|W(D_8)|}{|W(A_6)|} = 1024 \qquad N_7 = 2\frac{|W(D_8)|}{|W(A_7)|} = 256 \tag{5.51}$$

verifying (2.33). Similarly for $D(\omega_8/3)$ we have

$$N_d = \frac{|W(A_8)|}{|W(A_d \times A_{7-d})|} \qquad \text{for } 0 \leqslant d \leqslant 7. \tag{5.52}$$

Because $N_d = N_{7-d}$, (2.33) holds.

Table 10. The representative faces of $V(0)$ of the root lattice E_8 and their duals.

Face dimension	Diagram	Number of faces
7	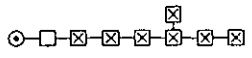	$2^4\,3\,5$
6	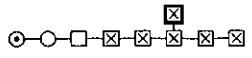	$2^6\,3\,5\,7$
5	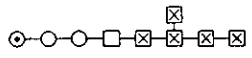	$2^6\,3^3\,5\,7$
4	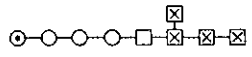	$2^8\,3^3\,5\,7$
3	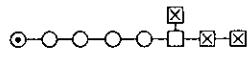	$2^9\,3^3\,5\,7$
2	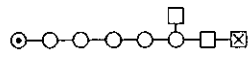	$2^9\,3^3\,5\,7$
1	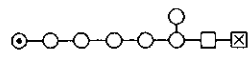	$2^9\,3^3\,5$
1	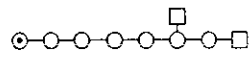	$2^{10}\,3^3\,5$
0	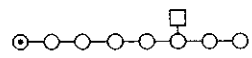	$2^7\,3^3\,5$
0	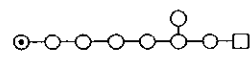	$2^4\,3^3\,5$

5.8. The root lattice F_4

Table 11 contains our results concerning the faces of $V(0)$ of the root lattice of F_4.

In the case of F_4 we have the highest long, and the highest short roots respectively given by

$$\begin{aligned}\xi &= 2\alpha_1 + 3\alpha_2 + 4\alpha_3 + 2\alpha_4 = \omega_1\\ \xi_s &= 2\alpha_1 + 4\alpha_2 + 3\alpha_3 + 2\alpha_4 = \omega_4.\end{aligned} \tag{5.53}$$

Dualization of the diagram produces the dual $\check{F}_4$ with long simple roots $\check{\alpha}_4$ and $\check{\alpha}_3$ and short simple roots $\check{\alpha}_2$ and $\check{\alpha}_1$. The highest long root of $\check{F}_4$ is

$$\check{\xi}_s = 2\check{\alpha}_4 + 3\check{\alpha}_3 + 4\check{\alpha}_2 + 2\check{\alpha}_1. \tag{5.54}$$

Therefore the boxes of the decorated diagram denote the points

$$\frac{\omega_1}{2}, \frac{\omega_2}{4}, \frac{\omega_3}{3}, \frac{\omega_4}{2}$$

and

$$F = \left\langle 0, \frac{\omega_1}{2}, \frac{\omega_2}{4}, \frac{\omega_3}{3}, \frac{\omega_4}{2} \right\rangle. \tag{5.55}$$

The vertices of $V(0)$ all belong to the single W-orbit represented by the point $\omega_4/2$.

Validity of Euler's formula is evident from the last column of table 11:

In this case we have $D(\omega_4/2)$ which is the 4-cross polytope with the symmetry group $W(C_4)$.

Table 11. The representative faces of $V(0)$ of the root lattice F_4 and their duals.

Face dimension	Diagram	Number of faces
3		$2^4\,3\,5$
2	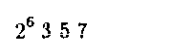	$2^6\,3\,5\,7$
1	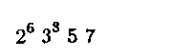	$2^6\,3^3\,5\,7$
0	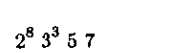	$2^8\,3^3\,5\,7$

5.9. The root lattice G_2

The pertinent results in this case have already been presented as part of an example in section 3 (cf figure 1). We add the same information here in the form of table 12 for completeness and uniformity of the presentation of our results.

For G_2 we have

$$\xi = 2\alpha_1 + 3\alpha_2 \qquad \xi_s = \alpha_1 + 2\alpha_2. \tag{5.56}$$

The G_2 diagram is self-dual, i.e. a dualization produces $\check{G}_2$. Its long simple root is $\check{\alpha}_2$ and the short simple one is $\check{\alpha}_1$. The highest long root is now

$$\check{\xi}_s = 2\check{\alpha}_2 + 3\check{\alpha}_1. \tag{5.57}$$

Consequently the boxes of the Coxeter–Dynkin diagram are the points $\omega_2/2$, $\omega_1/3$, and $F = \langle 0, \omega_2/2, \omega_1/3\rangle$.

Table 12. The representative faces of $V(0)$ of the root lattice G_2 and their duals.

Face dimension	Diagram	Number of faces
1		6
0		6

The Delaunay cell $D(\omega_2/2)$ has the symmetry of $W(A_2)$ and

$$N_0 = N_1 = \frac{|W(A_2)|}{|W(A_1)|} = 3$$

(cf figure 1 and (3.24)).

6. Generalized kaleidoscope

The solution to determining the Voronoi cells of a root lattice consists of describing the fundamental chamber of the affine Weyl group $W_a = W \ltimes Q$ by its Coxeter–Dynkin diagram and determining the rules by which the diagram is decorated into

two subdiagrams representing respectively a k-face of the Voronoi cell and its dual $(n-k)$-face. The dual faces are described using the Wythoff construction on the corresponding subdiagram. The root lattice Q itself can be viewed as an extreme case of the Wythoff construction when the entire Coxeter–Dynkin diagram is used for this purpose.

We can interpret the Coxeter–Dynkin diagram and the fundamental chamber as simply giving the reflecting hyperplanes for the generating reflections of W_a together with the angles between them. In general, a collection of reflecting hyperplanes which are situated so as to have all their mutual angles of intersection as submultiples of π, say π/m_{ij}, $m_{ij} \in \mathbb{Z}_+$, $i,j \in \{1,2,\ldots,n\}, i \neq j$, is called a *generalized kaleidoscope*. It can be represented by a Coxeter diagram, very much as before [C]. We introduce one node for each mirror and join nodes i and j by an edge overmarked with the number $m_{ij}(=m_{ji})$. If $m_{ij}=2$ we discard the edge, and in the case $m_{ij}=3$ we usually omit the marking. This leads us to generalize the situation at hand in two ways simultaneously:

(i) We may replace the Euclidean (or affine) kaleidoscope by any other, providing that it is a bounded simplex F of spherical, Euclidean, or hyperbolic geometry.

(ii) We may choose the special node of the corresponding Coxeter–Dynkin at will.

Denoting by W the group generated by the reflections in the walls of F and the vertex of F corresponding to the special node by v_0, we define the discrete set of points

$$Q := Wv_0.$$

Then Q plays a role analogous to the root lattice Q and we may consider its Voronoi regions (clearly all W-translates of each other), the facets of the Voronoi region, and the corresponding Delaunay cells and their facets. Remarkably the method we have described above works without any change in this new situation, except that the vertices of F can no longer be given using a system of marks $\{m_i\}$.

Here we confine ourselves to a few examples that illustrate some of the possibilities. By redefining the Voronoi cells in a way avoiding the metric, we can develop a theory that applies to any generalized kaleidescope and to any W-orbit of the Tits cone X. It is then possible to classify the facet structure of the Voronoi cells and their duals by a scheme of decorations of the Coxeter diagram that is a simple and natural generalization of the scheme developed here. The more general setting leads to an entirely different exposition of the classification. Details appear in [12].

6.1. A hyperbolic kaleidescope

Suppose we have given the diagram

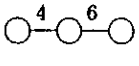

.

This represents the kaleidoscope generated by reflections in a triangle whose interior angles are $\pi/4, \pi/6, \pi/2$. Such a triangle exists only in the hyperbolic plane. The fundamental region F and some of its reflected images are shown in figure 3. We consider the set of points Q given by

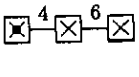

.

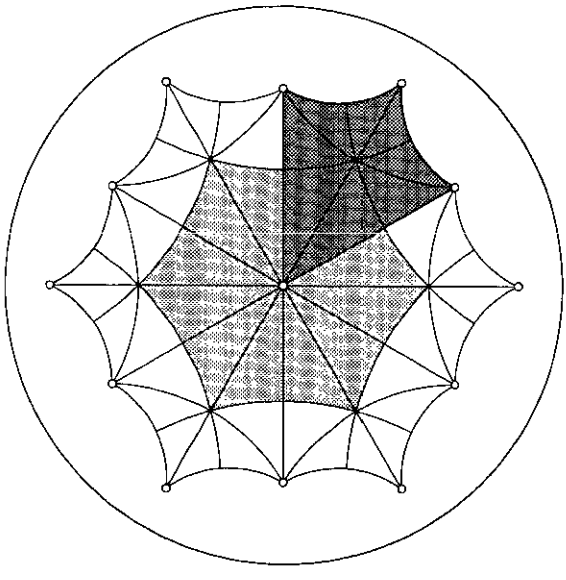

Figure 3. The kaleidoscope of section 6.1 is a tesselation of the hyperbolic plane by reflected images of a triangle whose angles are $\pi/2$, $\pi/4$, $\pi/6$. In the representation of the hyperbolic plane shown here the outer circle is the absolute circle at infinity and the geodesics are arcs of circles orthogonal to the absolute. Only a small part of the tesselation, which has infinitely many cells, is shown.

This means that we select the vertex v_0 of F corresponding to the dotted node and apply to it the entire reflection group.

The Voronoi region is then the hexagon

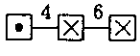

on figure 4 with edges and vertices and their duals given by the diagrams

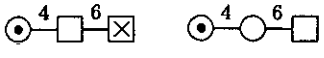

as illustrated in figure 4.

6.2. A spherical kaleidescope

Consider the diagram

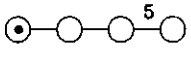

The full reflection group W here has order 14 400 [10]. For the set Q we take

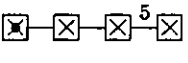

which consists of 14 400/120 = 120 points comprising the vertices of the well known 600 cell in 4-space. We view this as a tesselation of spherical 3-space. The Voronoi region V for Q is

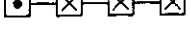

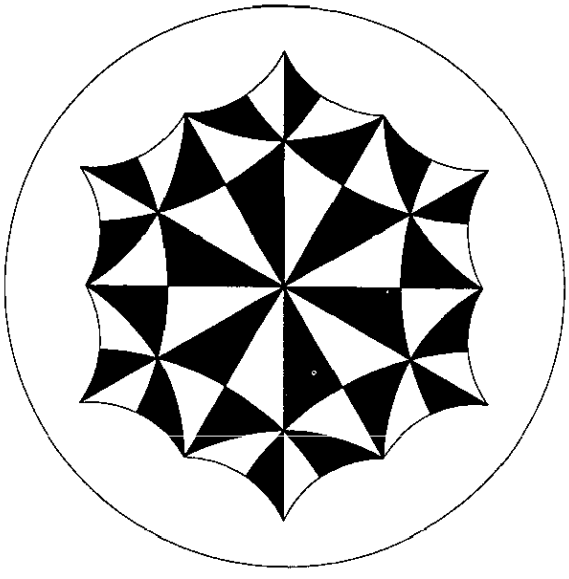

Figure 4. Voronoi and Delaunay cells of the hyperbolic kaleidoscope of section 6.1. The orbit under the reflection group of the centre point (indicated by open circles) gives rise to the typical Voronoi region shown as the hexagon in light shading. The quadrangle indicated by the dark shading is a typical Delaunay cell of maximum dimension.

with facets and duals given by the diagrams

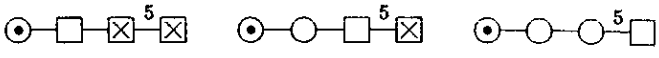

Using the fact that the reflections

generate a group of order 10, and counting the facets as before yields

$$N_2 = \frac{120}{10} = 12 \qquad N_1 = \frac{120}{2 \cdot 2} = 30 \qquad N_0 = \frac{120}{3!} = 20$$

from which it is obvious that V is a regular dodecahedron. The dual cells are all simplexes of various dimensions.

6.3. Two C_4 kaleidescopes

Finally let us consider two examples of type C_4 in which we assign the special role, indicated by the dotted circle, to different nodes of the diagram. We take

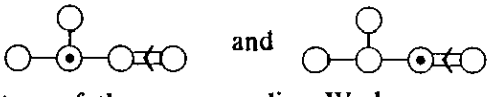

The structure of the corresponding Weyl groups, given by the subdiagrams of nodes without the dot, is $W(A_1 \times A_1 \times C_2)$ and $W(A_3 \times A_1)$. As the diagrams of the Voronoi domains we thus have respectively

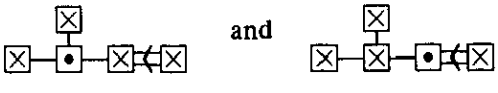

Table 13. Representative faces of Voronoi domains V of the two kaleidoscopes of section 6.3, their multiplicities, and dual faces (subdiagram of circles).

Face	Diagram	#	Diagram	#
V	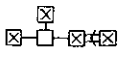	1	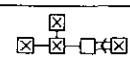	1
3-face	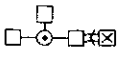	8	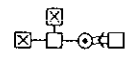	12
2-face	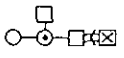	4	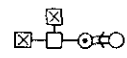	6
2-face	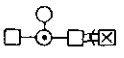	4	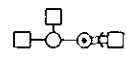	24
2-face	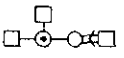	8		
1-face	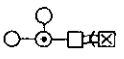	2	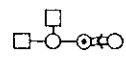	12
1-face	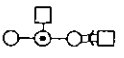	4	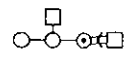	8
1-face	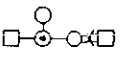	4	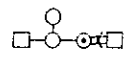	8
1-face	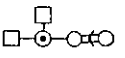	4		
0-face	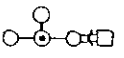	2	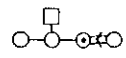	4
0-face	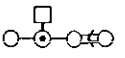	2	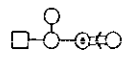	4
0-face	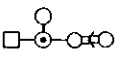	2	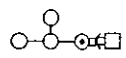	2

Using the same strategy as before, we find the representatives of W-orbits of faces, their multiplicities, and duals analogous to those shown in table 2. We have put together these results in table 13.

One may have noticed that we have, in fact, already considered kaleidoscopes with special nodes elsewhere than on the extension node. Indeed, these were the cases where we were interested in the structure of Delaunay domains or facets of facets (see, for example, the diagrams in (3.28) and (5.7)).

Acknowledgments

We would like to acknowledge conversations with Drs P Kramer, L Michel, and A Janner which stimulated our interest in this problem. We also acknowledge the hospitality of the Theory Division of the Los Alamos National Laboratory where the manuscript was completed.

The work was partially supported by the Natural Sciences and Engineering Research Council of Canada, the Fonds FCAR du Québec, and by the Killam Research Fellowship (JP).

References

[1] Voronoi G 1908 Nouvelles applications des paramètres continus à la théorie des formes quadratiques *J. reine ang. Math.* **133** 97–178; 1908 **134** 198–297; 1909 **136** 67–181

[2] Delaunay (or Delone) B N 1933 Neue Darstellung der geometrischen Kristallographie *Z. Krist.* 84 109–49

[3] Baake M, Joseph D, Kramer P and Schlottmann M 1990 Root lattices and quasicrystals *J. Phys. A: Math. Gen.* **23** L1037–41

Baake M, Kramer P, Schlottman M and Zeidler D 1990 Planar patterns with fivefold symmetry as sections of periodic structures in 4-space *Int. J. Mod. Phys.* **B-4** 2217–68

Kramer P, Papadopolos Z and Zeidler D 1992 The root lattice D_6 and icosahedral quasicrystals *Proc. Symp. Symmetries in Physics (Cocoyoc, Mexico 1991) AIP Conference Proc.* ed A Frank *et al* to appear

Kramer P and Schlottmann M 1989 Dualization of Voronoi domains and Klotz construction: a general method for the generation of proper space fillings *J. Phys. A: Math. Gen.* **22** L1097–102

[4] Baake M, Joseph D and Schlottmann M 1991 The root lattice D_4 and planar quasilattices with octagonal and dodecagonal symmetry *Int. J. Mod. Phys.* **B-5** 1927–53

[5] Conway J H and Sloane N J A 1988 *Sphere Packings, Lattices and Groups* (New York: Springer)

[6] Conway J H and Sloane N J A 1991 The cell structures of certain lattices *Miscellanea Mathematica* ed P Hilton, F Hirzebruch and R Remmert (New York: Springer)

[7] Brown H, Bülow R, Neubüser J, Wondratschek H and Zassenhaus H 1978 *Crystallographic Groups of Four-dimensional Space* (New York: Wiley)

[8] Whittaker E J W 1978 *An Atlas of Hyperstereograms of the Four-dimensional Crystal Classes* (Oxford: Clarendon)

[9] Senechal M 1992 Introduction to lattice geometry *From Number Theory to Physics* ed P Mousa and M Waldschmidt (New York: Springer) to appear

[10] Coxeter H S M 1973 *Regular Polytopes* (New York: Dover)

[11] Bourbaki N 1968 *Groupes et algèbres de Lie, Éléments de mathématiques* (Paris: Hermann) ch 4–6

[12] Moody R V and Patera J 1992 Voronoi domains and dual cells in the generalized kaleidoscope with applications to root and weight lattices *Preprint* CRM-1803, 50p (submitted to *Inventiones Math.*)

[13] Moody R V and Pianzola A 1992 *Lie Algebras with Triangular Decompositions* (New York: Wiley) to appear

[14] McKay W G, Patera J and Rand D 1990 *Tables of Representations of Simple Lie Algebras* (Montréal: Les Publications CRM, Université de Montréal)